Agricultural and Forest Meteorology 326 (2022) 109178

Contents lists available at ScienceDirect

Agricultural and Forest Meteorology

journal homepage: www.elsevier.com/locate/agrformet

Hyperspectral response of agronomic variables to background optical variability: Results of a numerical experiment

Lin Gao [a], Roshanak Darvishzadeh [b], Ben Somers [c], Brian Alan Johnson [d], Yu Wang [e], Jochem Verrelst [f], Xiaofei Wang [a,*], Clement Atzberger [g]

[a] College of Geography and Environment, Shandong Normal University, Jinan 250014, China
[b] Faculty of Geo-Information Science and Earth Observation (ITC), University of Twente, P.O. Box 217, 7500 AE Enschede, the Netherlands
[c] Division Forest, Nature and Landscape, Department Earth and Environmental Sciences, KU Leuven, Celestijnenlaan 200E-2411, Leuven B-3001, Belgium
[d] Institute for Global Environmental Strategies, Hayama, Kanagawa 240-0115, Japan
[e] School of Surveying and Land Information Engineering, Henan Polytechnic University, Jiaozuo 454000, China
[f] Image Processing Laboratory (IPL), Parc Científic, Universitat de València, Paterna 46980, Spain
[g] Institute of Geomatics, University of Natural Resources and Life Sciences (BOKU), Vienna 1090, Austria

ARTICLE INFO

Keywords:
Hyperspectral response
Global sensitivity analysis
Leaf chlorophyll content
Leaf area index
Soil type
Non-photosynthetic vegetation

ABSTRACT

Understanding how biophysical and biochemical variables contribute to the spectral characteristics of vegetation canopies is critical for their monitoring. Quantifying these contributions, however, remains difficult due to extraneous factors such as the spectral variability of canopy background materials, including soil/crop-residue moisture, soil-type, and non-photosynthetic vegetation (NPV). This study focused on exploring the spectral response of two important agronomic variables (1) leaf chlorophyll content (C_{ab}) and (2) leaf area index (LAI) under various canopy backgrounds through a global sensitivity analysis of wheat-like canopy spectra simulated using the physically-based PROSAIL radiative transfer model. Our results reveal the following general findings: (1) the contribution of each agronomic variable to the simulated canopy spectral signature varies considerably with respect to the background optical properties; (2) the influence of the soil-type and NPV on the spectral response of canopy to C_{ab} and LAI is more significant than that caused by soil/crop-residue moisture; (3) spectral bands at 560 and 704 nm remain sensitive to C_{ab} while being least affected by the impacts of variations in the NPV, soil-type and moisture; (4) the near-infrared (NIR) spectral bands exhibit higher sensitivity to LAI and lower background effects only in the cases of soil/crop-residue moisture but are relatively strongly affected by soil-type and NPV. Comparative analysis of the correlations of twelve widely used vegetation indices with agronomic variables indicates that LICI (LAI-insensitive chlorophyll index) and Macc01 (Maccioni index) are more effective in estimating C_{ab}, while OSAVI (optimized soil adjusted vegetation index) and MCARI2 (modified chlorophyll absorption ratio index 2) are better LAI predictors under the simulated background variability. Overall, our results highlight that background reflectance variability introduces considerable differences in the agronomic variables' spectral response, leading to inconsistencies in the VI- C_{ab} /-LAI relationship. Further studies should integrate these results of spectral responsivity to develop trait-specific hyperspectral inversion models.

1. Introduction

Plants are an essential component of the terrestrial ecosystem. Leaf area index (LAI), as an indicator of vegetation growth (Ma *et al.*, 2018), and the leaf chlorophyll content (henceforward referred to as C_{ab}), as an indicator of the photosynthetic capacity of vegetation (Croft *et al.*, 2017), are two of the most important vegetation variables that control water, energy and carbon exchange processes in the terrestrial biosphere. Knowledge of the spatial distribution of the LAI and C_{ab} is therefore crucial to assess the terrestrial carbon and water balance and to forecast agricultural yield, especially facing the challenges of global change (Chen *et al.*, 2019; Gitelson *et al.*, 2003; Houborg *et al.*, 2013; Huang *et al.*, 2015). Remote sensing can provide such information by enabling the non-destructive estimation of LAI and C_{ab} at regional to

* Corresponding author.
E-mail address: wangxiaofei_nju@163.com (X. Wang).

https://doi.org/10.1016/j.agrformet.2022.109178
Received 28 February 2022; Received in revised form 18 September 2022; Accepted 19 September 2022

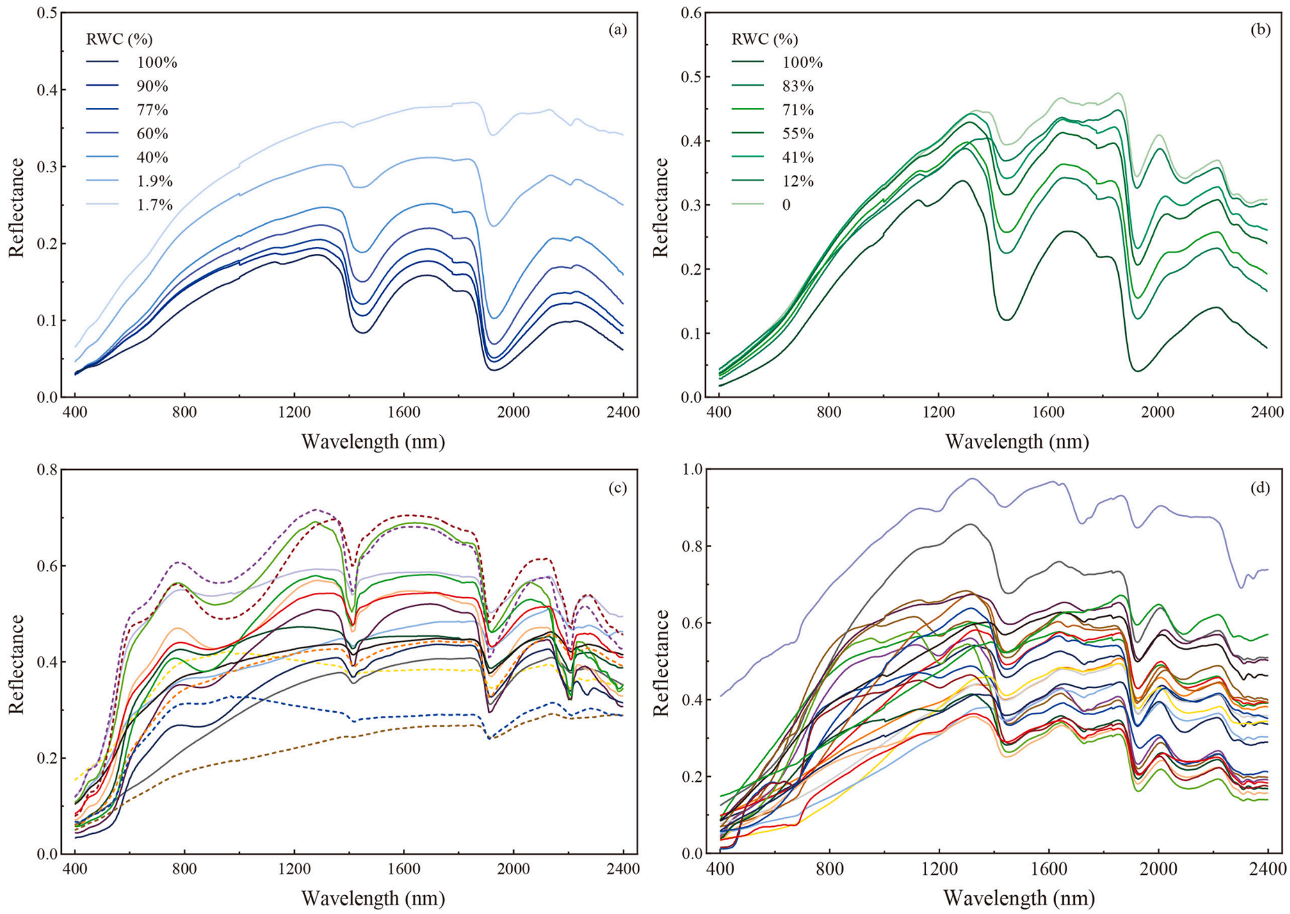

Fig. 1. Reflectance spectra of 55 backgrounds used as input into the PROSAIL model: (a) bare soil at seven different relative water contents (RWC), (b) crop residue with seven different levels of moisture content, (c) 17 contrastive soil types, and (d) 24 NPV.

global scales (Croft *et al.*, 2020; Fang *et al.*, 2019). The retrieval of LAI and C_{ab} from remote sensing data relies on the fact that the optical properties of leaves and the canopy correlate strongly with vegetation amount and leaf composition (Asner, 1998; Jacquemoud *et al.*, 2009). Consequently, an in-depth understanding of how the LAI and C_{ab} determine the vegetation spectral behavior – including vegetation indices (VIs) – under the effects of external factors is vital for a more accurate estimation of LAI and C_{ab} from remote sensing data. In this respect, the effects of changing soil background characteristics deserve more attention as, generally, even within a small agricultural field, the background optical properties vary spatially and temporally (Baret and Guyot, 1991; Li *et al.* 1993). Such spatiotemporal variations in background reflectance are the main source of uncertainty in satellite-derived LAI or C_{ab} products (Darvishzadeh *et al.*, 2008a, 2019; Eitel *et al.*, 2009; Verrelst *et al.* 2010).

Numerous studies have used simulations based on radiative transfer models (RTMs) to analyze the sensitivity of surface reflectance of a soil-vegetation system, usually through either local sensitivity analysis (LSA) or global sensitivity analysis (GSA) methods. LSA involves the qualitative analysis of the relationships between the spectral characteristics and a specific biophysical or biochemical parameter while keeping the remaining variables fixed. This has been successfully applied to evaluate the spectral sensitivity of agronomic variables to different soil types and water contents (Bach and Verhoef, 2003; Díaz and Blackburn, 2003; Huete *et al.* 1985; Morcillo-Pallarés *et al.*, 2019). However, LSA cannot identify and quantify the influential and noninfluential variables – and their mutual interdependences – that govern the spectral signatures at different wavelengths over the entire input variable space (Saltelli and Annoni, 2010). Such assessments have important implications for selecting optimal wavelengths for the estimation of LAI and C_{ab}. Moreover, previous applications of LSA rarely included the spectral response in the shortwave infrared (SWIR) bands that are configured in popular satellite sensors (e.g., Landsat-8 OLI, Sentinel-2 MSI) and commonly used for LAI retrievals (Amin *et al.*, 2021; Dong *et al.*, 2020). By contrast, GSA quantifies simultaneously the contribution of various model input parameters to the reflected electromagnetic radiation (Gu *et al.*, 2016; Mousivand *et al.*, 2014; Wang *et al.*, 2019; Xiao *et al.*, 2014), and is therefore typically preferable over LSA. In previous studies, however, GSA has often ignored the sometimes high spatiotemporal variability in the background optical properties.

To gain maximum understanding, sensitivity analyses should include major factors which contribute to the spectral variability of background materials. Typically, in many agricultural ecosystems, the background spectrum is highly heterogeneous due to different soil types, organic carbon contents, fertilizer treatments, amounts and type of non-photosynthetic vegetation (NPV, e.g., crop residue, litter, senescent grass), and surface water and roughness status. Therefore, it is imperative to better elucidate the spectral response of vegetation variables under different background conditions.

The objectives of this paper are: (1) to quantify the contributions of LAI and C_{ab} to the full-wavelength spectral response (400–2400 nm), as well as to commonly available VIs, when background optical properties are variable, and (2) to determine the spectral regions where LAI and/or C_{ab} most strongly affect the canopy spectral characteristics while being minimally influenced by variations in background reflectance. To address these goals, extensive numerical experiments based on radiative transfer simulations were conducted to generate representative spectral datasets. Research objectives were investigated for a setting simulating

Table 1
Main variables of PROSAIL in the global sensitivity analysis. In bold, the eight non-fixed variables of interest.

Variable	Symbol	Unit	Range	Refs.
Leaf structure parameter	N	-	1.0-2.5	Liu *et al.* (2012)
Leaf chlorophyll content	C_{ab}	$\mu g/cm^2$	5-100	Xu *et al.* (2019)
Leaf carotenoid content	C_{xc}	$\mu g/cm^2$	8	Liang *et al.* (2015)
Brown pigment content	C_{bp}	-	0	Xu *et al.* (2019)
Equivalent water thickness	C_w	cm	0.0043-0.0713	Feret *et al.* (2011)
Dry matter content	C_m	g/cm^2	0.0008-0.0331	Feret *et al.* (2011)
Leaf area index	LAI	m^2/m^2	0.1-10	Liang *et al.* (2015)
Average leaf inclination angle	ALA	°	30-80	Verger *et al.* (2014)
Hot-spot parameter	S_L	-	0.2	Xiao *et al.* (2014)
Background brightness factor	α	-	0-1	Verrelst et al. (2015b)
Solar zenith angle	θ_s	°	20-60	-
Viewing zenith angle	θ_v	°	0	-
Relative azimuth angle	φ_{sv}	°	0	-
Fraction of diffuse incoming solar radiation	*skyl*	-	0.1	Zhang *et al.* (2016)

wheat canopies (*Triticum aestivum* L.) as well as other continuous crop canopies similar to wheat.

2. Materials and methods

2.1. Background spectra

Mimicking vegetation spectra with variable backgrounds requires realistic spectra from background materials and appropriate canopy reflectance models. Spectral reflectance of various soil types in China were collected from (i) a subset of the ICRAF-ISRIC spectral library (the International Centre for Research in Agroforestry-International Soil Reference and Information Centre) as described by Garrity and Bindraban (2004), and (ii) the CSSL spectral library (the Chinese Soil Spectral Library) described in Shi et al. (2014). The ICRAF-ISRIC spectral library includes 245 soil profiles collected from 47 locations in China. The CSSL spectral library contains 1581 soil samples derived from 16 soil groups of the Genetic Soil Classification of China (GSCC). Fifty-one reflectance spectra of NPV were acquired from the ECOSTRESS spectral library (the ECOsystem Spaceborne Thermal Radiometer Experiment on Space Station, see Meerdink *et al.*, 2019 for details). To avoid data redundancy caused by similar soil or NPV spectra in these three independent spectral libraries and to better sample the feature space, we used the spectral angle mapping classification method (Kruse *et al.*, 1993) to identify several representative spectra based on the following equation:

$$\alpha_{XY} = \cos^{-1}\left[\frac{\sum_{i=1}^{n}(x_i y_i)}{\sqrt{\left(\sum_{i=1}^{n} x_i^2\right)} \times \sqrt{\left(\sum_{i=1}^{n} y_i^2\right)}}\right]$$

where, $X = (x_1, x_2, \ldots, x_n)$ and $Y = (y_1, y_2, \ldots, y_n)$ are two different soil spectral vectors with n wavebands; α_{XY} is the spectral angle between X and Y and ranges from 0 to $\pi/2$ ($\alpha_{XY} = 0$ means that X and Y are completely similar, while $\alpha_{XY} = \pi/2$ means that X and Y are entirely different).

Using the criterion that two different spectra with a spectral angle $\alpha < 0.05$ would be identified as similar reflectance (Jia *et al.*, 2016), the spectral reflectance curves of 1826 soil and 51 NPV were classified into 17 soil and 24 NPV groups, respectively. In addition, a set of average spectra generated from a dataset containing 70 crop-residue and soil at seven moisture levels (Quemada and Daughtry, 2016) was used to mimic the canopy spectral variation due to differences in water contents of the ground underneath the canopy. In total, 55 different background reflectance spectra were assessed (Fig. 1): 17 soil types, 24 NPV, 7 soil moisture contents, and 7 crop-residue moisture contents. The chosen background spectra display highly distinct spectral contrast linked to soil type, composition, texture, and surface conditions, which permits to assess the impacts of a wide range of natural backgrounds. As a limitation it has to be noted however that the spectra come from different sources and are not mutually inclusive – in particular the (hypothetical) averages of the subsets (a) to (d) in Fig. 1 would not match each other.

2.2. Global sensitivity analysis

We used the extended Fourier amplitude sensitivity test method (EFAST, Saltelli *et al.*, 2008), implemented in the software package SimLab (ver. 2.2, SIMLAB, 2009) to perform the global sensitivity analysis of the simulated datasets. The EFAST is a variance-based GSA method which has recently gained wider attention in agricultural modeling (Jin *et al.*, 2018; Xu et al., 2019). The sensitivity measures of EFAST include the first-order sensitivity index S_i, which reflects the individual contribution of each input parameter to the model output, and the total-order sensitivity index ST_i, which represents the overall contribution of each parameter to the model output (including interactions between each parameter and the remaining parameters). Both sensitivity indices can be expressed as follow:

$$S_i = \frac{V_i}{V}$$

$$ST_i = S_i + \sum_{j \neq i} S_{ij} + \cdots + S_{1,2,\ldots,k}$$

where V_i ($V_i = V[E(Y|x_i)]$) represents the first-order variance for each input factor; V is the attribution of total output variance and calculated according to $V = \sum_{i=1}^{k} V_i + \sum_{i=1}^{k} \sum_{j>i}^{k} V_{ij} + \cdots + V_{1,2,\ldots,k}$; and V_{ij} ($V_{ij} = V[E(Y|x_i, x_j)] - V_i - V_j$) to $V_{1,2,\ldots,k}$ represent the interactions among k factors (see Saltelli *et al.*, 2010, for further details on EFAST).

To investigate the spectral response of agronomic variables with different background scenarios, the EFAST global sensitivity analysis was performed using simulations with the well-known radiative transfer model PROSAIL (Berger *et al.*, 2018; Jacquemoud *et al.*, 2009) that could produce nadir-viewed canopy reflectance (from 400 to 2400 nm in 1 nm increments), assuming negligible atmospheric effects. The MATLAB code for PROSAIL can be downloaded at http://teledetection.ipgp.jussieu.fr/prosail/. To parameterize the PROSAIL model in a plausible manner, a combination of (i) *prior* knowledge (Liu *et al.*, 2012; Verger *et al.* 2014; Xu et al., 2019; Zhang *et al.* 2016) from site-specific information gathered in field campaigns of wheat, and (ii) related published literature (Feret *et al.*, 2011; Liang *et al.*, 2015; Xiao *et al.*, 2014) were used to assign the specific ranges of the main model input variables of wheat-like canopies (Table 1). All parameters were varied independently as information about possible covariation was not available.

For an informative sensitivity analysis, the sample size of input parameters should be as large as possible. On the other hand, the computational costs of the simulation increase with sample size. To assess how sample size affects the convergence of the sensitivity indices, we ran a set of the EFAST global sensitivity analysis with a gradually increasing sample size and then computed the total-order sensitivity index of the widely-used NDVI (normalized difference vegetation index) based on the narrowband reflectance at 670 and 800 nm from PROSAIL simulations, corresponding to eight variables. Substantial variations in the total-order sensitivity index of each input parameter of the PROSAIL model were observed when the sample size is $\leq$ 10 000 while it is more stable for a sample size of 30 000 (Fig. 2). As no more fluctuations occurred after 35 000 simulations, a final sample size of 40 000 samples

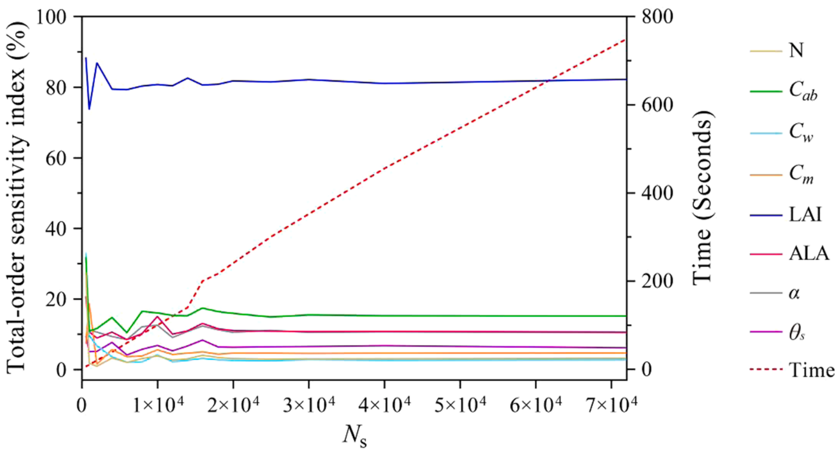

Fig. 2. Analysis of the impact of the total number of samples (N_s) on the stability of global sensitivity analysis for NDVI with PROSAIL based on the extended Fourier amplitude sensitivity test.

Table 2
A set of vegetation indices examined in this paper

Spectral index	Formulation	Estimation or Elimination	Refs.
MSAVI, Modified soil adjusted vegetation index	$0.5[2R_{800}+1-\sqrt{(2R_{800}+1)^2-8(R_{800}-R_{670})}]$	Background effect	Qi *et al.* (1994)
OSAVI, Optimized soil adjusted vegetation index	$(1+0.16)(R_{800}-R_{670})/(R_{800}+R_{670}+0.16)$	Background effect	Rondeaux *et al.* (1996)
NDVI, Normalized difference vegetation index	$(R_{800}-R_{670})/(R_{800}+R_{670})$	LAI	Rouse *et al.* (1974)
MSR, Modified simple ratio	$[(R_{800}/R_{670})-1]/\sqrt{(R_{800}/R_{670})+1}$	LAI	Chen (1996)
MCARI2, Modified chlorophyll absorption ratio index 2	$\frac{1.5[2.5(R_{800}-R_{670})-1.3(R_{800}-R_{550})]}{\sqrt{(2R_{800}+1)^2-(6R_{800}-5\sqrt{R_{670}})-0.5}}$	LAI	Haboudane *et al.* (2004)
sLAIDI, Standardized LAI Determining Index	$S(R_{1050}-R_{1250})/(R_{1050}+R_{1250})$, where $S=5$	LAI	Delalieux *et al.* (2008)
CI_{RE}, Red-edge chlorophyll index	$(R_{750}/R_{710})-1$	Chlorophyll	Gitelson *et al.* (2006)
MTCI, MERIS terrestrial chlorophyll index	$(R_{754}-R_{709})/(R_{709}-R_{681})$	Chlorophyll	Dash and Curran (2004)
Macc01, Maccioni index	$(R_{780}-R_{710})/(R_{780}-R_{680})$	Chlorophyll	Maccioni *et al.* (2001)
LICI, LAI-insensitive chlorophyll index	$(R_{735}/R_{720})-[(R_{573}-R_{680})/(R_{573}+R_{680})]$	Chlorophyll	Li *et al.* (2020)
$MCARI_{(705,\ 750)}/OSAVI_{(705,\ 750)}$	$\frac{[(R_{750}-R_{705})-0.2(R_{750}-R_{550})]\left(\frac{R_{750}}{R_{705}}\right)}{\left[\frac{(1+0.16)(R_{750}-R_{705})}{R_{750}+R_{705}+0.16}\right]}$	Chlorophyll	Wu *et al.* (2008)
PRI, Photochemical reflectance index	$(R_{531}-R_{570})/(R_{531}+R_{570})$	Photosynthetic efficiency	Gamon *et al.* (1992)

was selected to distinguish between influential and noninfluential parameters. Thus, a total of 40 000 combinations of the eight model parameters (N, C_{ab}, C_w, C_m, LAI, ALA, α, θ_s) were randomly generated (following uniform distribution) within the predefined ranges by using EFAST, resulting in the generation of 40 000 canopy spectra by running PROSAIL in the forward mode. Contrary to Widlowski *et al.* (2015), in the simulations, effects of leaf/canopy clumping were not considered, nor were the effects of background anisotropy. Then, the influence of the background on the contribution of C_{ab} and LAI to canopy reflectance as well as the twelve VIs selected (given in Table 2) was examined by repeatedly running EFAST for each of the 55 background spectra (i.e., 7 soil moisture contents + 7 crop-residue moisture contents + 17 soil types + 24 NPV types).

Furthermore, assuming measured canopy radiance with a black background is theoretically controlled by the scattering properties of the vegetation layer only, “pure” vegetation spectra were generated by inserting “zero” for background reflectance in the simulation (Jean-Baptiste Feret, personal communication; Gao *et al.*, 2000). Note that this is equivalent to a canopy bounded by a fully absorbing background (Shabanov *et al.*, 2000). The global sensitivity of pure vegetation spectra and their VIs (termed “pure” VI hereafter), was also calculated. Then, a comparison between the spectral response of a canopy with a scattering background (e.g., impacted by soil-type, soil moisture, NPV, crop-residue moisture) and that with a non-reflecting – and hence non-interfering – background, was studied to gain insight into how variation in the spectral response of agronomic variables owned solely to vegetation elements (see Appendix A for interested reader, not shown here for brevity).

3. Results

3.1. Variations of canopy spectral signatures to chlorophyll and LAI for different background optical properties

The background-induced changes in the canopy’s spectral response to C_{ab} and LAI are shown in Fig. 3 based on the mean and the standard deviation (sd) of the S_i criterion. Differences in S_i at a certain wavelength (as displayed by sd) reveal how much the contribution of the two agronomic variables (C_{ab} and LAI) varies, owing to background variability. Although canopy reflectance around 530–590 nm and around 690–710 nm is generally more sensitive to C_{ab} than in other spectral regions, the same spectral regions are also closely affected by background variations, not yet well described in the literature. We found that, due to the variability of background spectra, the leaf-level chlorophyll-sensitive wavebands in the visible and red-edge regions of the spectrum are altered. For example, spectral bands of high sensitivity to C_{ab} appear near 560 and 704 nm for variations in soil-type, near 570 and 700 nm for NPV, and near 595 and 695 nm for variations in soil or crop-residue moisture content (Fig. 3a). On the other hand, the impact of variations in backgrounds relative to C_{ab} at 560 and 704 nm is less strong compared to the impacts on other peak positions. Consequently, the use of canopy reflectance at 560 and 704 nm as predictors of C_{ab} estimates is

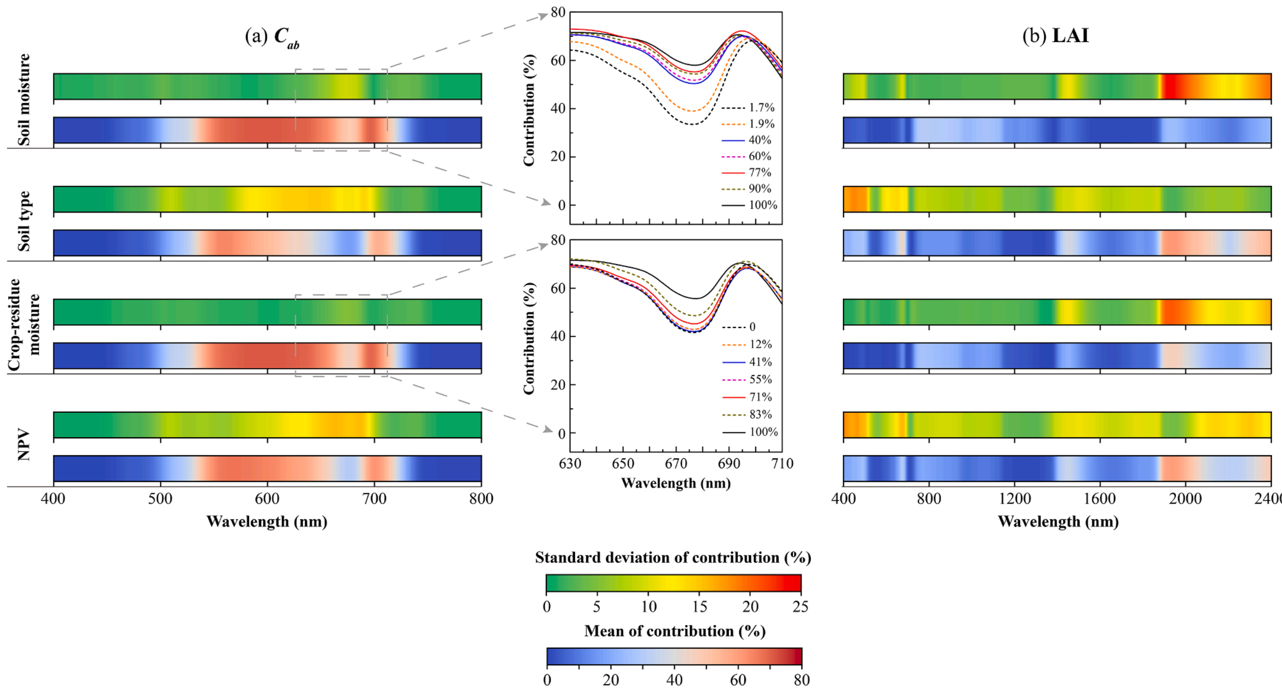

Fig. 3. The first-order sensitivity indices with associated error (mean ± standard deviation) of hyperspectral canopy reflectance to (a) C_{ab} and (b) LAI for 55 different background scenarios, including soil-type, soil moisture, NPV, and crop-residue moisture. Higher (lower) values of standard deviation indicate larger (less) disturbing effects of the respective background. Note that the S_i of canopy reflectance is restricted to 400 to 800 nm for C_{ab} as chlorophyll is transparent to infrared radiation (Knipling 1970).

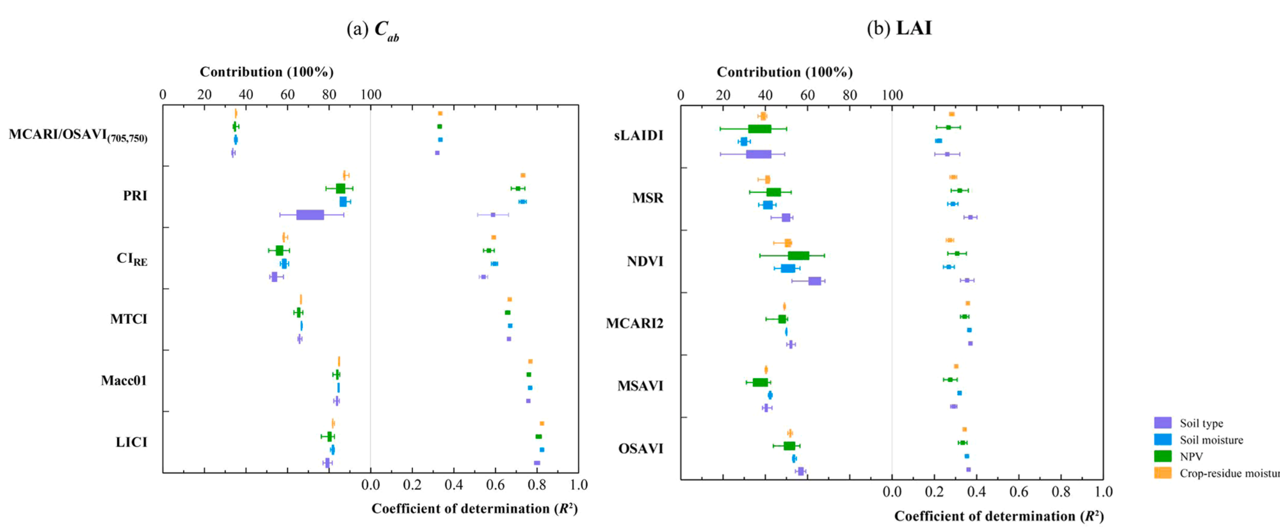

Fig. 4. The first-order sensitivity indices (S_i) as measures of the VIs response to C_{ab} and LAI using global sensitivity analysis and the coefficient of determination (R^2) for the relationships between VIs and C_{ab} and LAI based on the synthetic datasets. The left panels represent the boxplots of S_i, and the right panels are error bars of R^2 denoting the standard error in the mean across 55 different background scenarios.

desirable. This finding provides powerful support for spatially explicit monitoring of chlorophyll content using Sentinel-2 data, which have green and red-edge bands with center wavelengths of 560 and 704 nm, respectively. The canopy reflectance around 680 nm, which matches the chlorophyll absorption peaks, is closely related to C_{ab} only when considering variations in background moisture but is strongly affected by soil-type and NPV. Importantly, the sensitivity of canopy reflectance around 680 nm to C_{ab} decreases with increasing background moisture.

The impacts of background spectral properties on the response of canopy reflectance to changes in LAI vary with wavelength. As shown in Fig. 3b, spectral variations associated with soil-type and NPV impose a greater influence on the LAI-related spectral response of the spectral windows 450–530, 630–690 and 774–900 nm than does soil or crop-residue moisture. For instance, at the pigment-absorption features (around 487 and 675 nm) LAI explains 28% ± 18% and 44% ± 12% (when varying soil types) and 26% ± 16% and 30% ± 16% (when varying NPV) of variations in canopy reflectance, respectively, as opposed to 5% ± 10% and 10% ± 10% (when varying soil moisture) and 3% ± 3% and 13% ± 5% (when varying crop-residue moisture), respectively. Furthermore, canopy spectral response in the NIR range (774–900 nm) to LAI over background cases of soil-type and NPV is less strong than the response with a more or less wet background. In contrast, in the range 1900–2400 nm, differences in soil or crop-residue moisture affect the spectral response to LAI more than differences in soil

Table 3
The maximum sensitivity (mean ± sd) of canopy reflectance at different spectral regions to variations of leaf-level chlorophyll content based on EFAST.

Canopy background	Visible region Wavelength (nm)	Contribution (%)	Red-edge region Wavelength (nm)	Contribution (%)
Soil-type	560	64 ± 6	704	56 ± 7
Soil moisture	595	71 ± 1	695	70 ± 2
NPV	570	67 ± 7	700	62 ± 8
Crop-residue moisture	595	71 ± 1	695	69 ± 1
Fully absorbing background	585	62	695	62

types, particularly at water absorption features (around 1930 nm).

3.2. Sensitivities and correlations of VIs for various backgrounds

The response of VIs to background variations requires focal attention as VIs are extensively applied in the large-scale retrieval of vegetation variables. Fig. 4 visualises the sensitivities of different VIs to variations in leaf chlorophyll content or LAI and the correlations between agronomic variables and the VIs under all scenarios. In general, background influences from soil-type and NPV result in relatively high uncertainties in the C_{ab}-VIs relationships derived from simulations, while the effect of background moisture variability is minor (Fig. 4a) since the arithmetic combination of spectral bands employed in these chlorophyll-related indices reduce the effects of background moisture. The PRI remains highly sensitive to C_{ab} for all backgrounds except soil-type, in which the resulting PRI exhibits the worst performance with 13% interquartile range (IQR) of S_i and the coefficient of determination (R^2) of 0.59 ± 0.07 (mean ± sd). The CI_{RE} is slightly less sensitive to changes in C_{ab} (S_i =

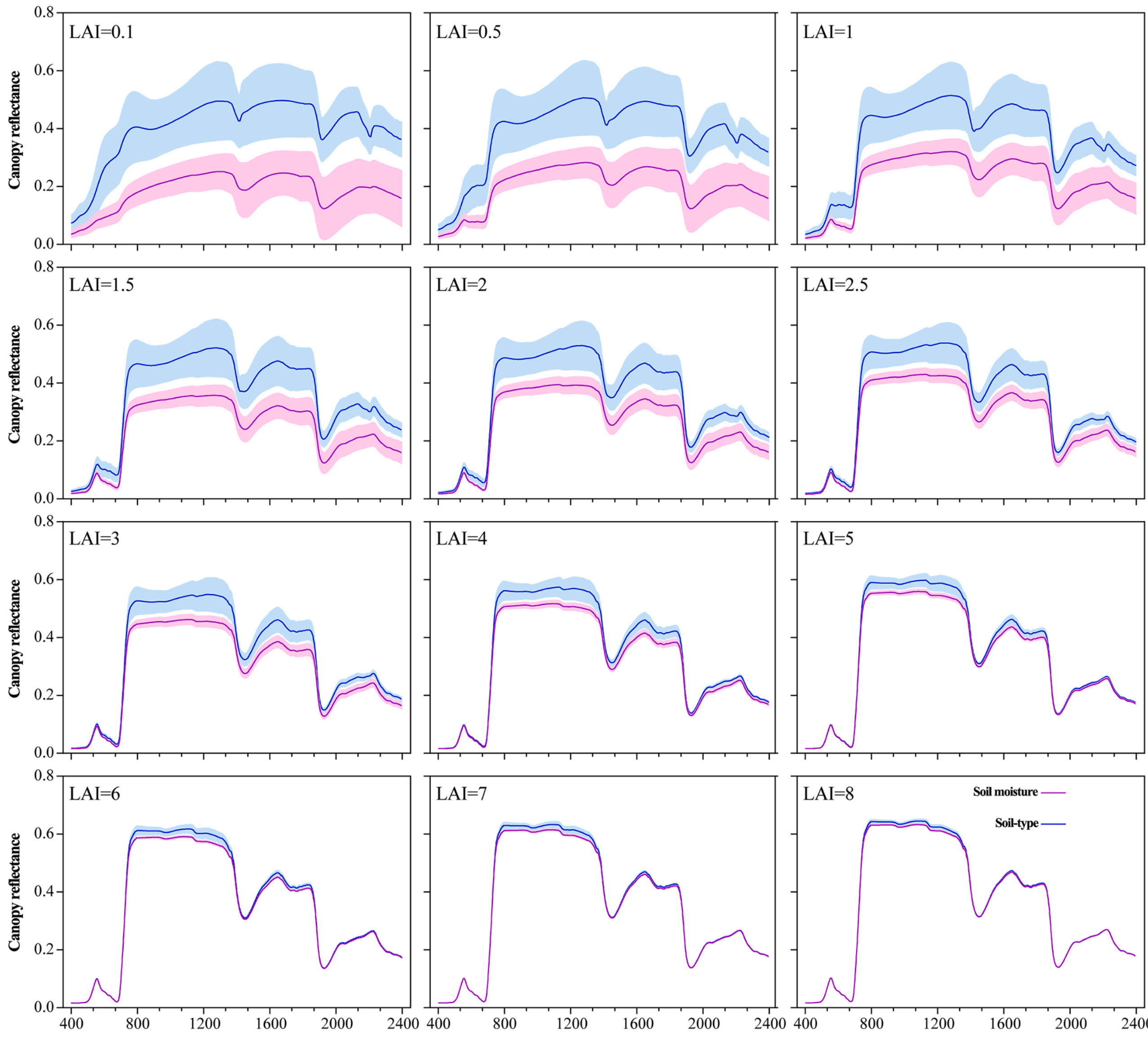

Fig. 5. The modelled influences of soil type or moisture on canopy reflectance for twelve canopy densities (LAI = 0.1, 0.5, 1, 1.5, 2, 2.5, 3, 4, 5, 6, 7, 8) based on PROSAIL. The distributions of all other PROSAIL parameters are kept constant (i.e., N = 1.5; $C_{ab} = 25\ \mu g/cm^2$; $C_{xc} = 8\ \mu g/cm^2$; $C_{bp} = 0$; $C_w = 0.01$ cm; $C_m = 0.004$ g$/cm^2$; ALA = 57°; $\theta_s = 37°$), and only the set of background spectra is changed according to Fig. 1. The light-colored areas depict the variations in the canopy reflectance with background variability.

56% ± 3%), and is moderately closely related to C_{ab} (R^2 = 0.57 on average), followed by MCARI/OSAVI$_{(705,\ 750)}$ with the lowest S_i of 34% ± 1% and R^2 of 0.33 (on average). It is worth noting that the MCARI/OSAVI$_{(705,\ 750)}$ response to C_{ab} is only slightly affected by background variability, partly attributed to the OSAVI-based 705 nm feature. By contrast, Macc01 and LICI are better estimators of chlorophyll content across various background conditions, as evidenced by the relatively higher sensitivity (S_i > 79% on average) and better relationships with C_{ab} (R^2 > 0.75 on average), followed by MTCI with S_i of 66% ± 1% and R^2 of 0.66 (on average). In theory, the LICI is recognized to be independent of LAI (Li *et al.*, 2020) with only a marginal S_i (< 1%, see Fig. B illustrating the GSA results for each of the selected VIs) that is lower compared to Macc01 with average S_i = 4%, and hence is the most robust chlorophyll-related index of the VIs tested here.

Compared to the chlorophyll-related indices, background optical variability more strongly influences the LAI-related indices (Fig. 4b). Specifically, the strong impacts of background optical properties on LAI quantifications using VIs are to be expected in agricultural land with contrastive soil types and NPV. On the contrary, the effects of varying moisture contents are a much less concern.

The different responses of NDVI to LAI with varying soil moisture (with IQR of about 6%) indicate that NDVI is subject to variability associated with soil brightness (Huete, 1988; Huete and Tucker, 1991). Background influences from soil-type and NPV, aside from brightness, also cause more differences in the responsiveness of NDVI to LAI (with IQR of about 8% on average), and so does MSR (with IQR of about 6.8% on average). For this reason, the NDVI-LAI relationships vary significantly among different canopy backgrounds (R^2 varied from 0.2 to 0.4). These outcomes partly explain the inconsistency of many experimental NDVI-LAI relationships, especially for seasonal crop growth monitoring at a global scale (Liu *et al.*, 2012; Liu and Huete, 1995; Xu *et al.*, 2020). Although the sLAIDI is little affected by the interference of chlorophyll effects (with minimal S_i < 0.01%) and yielded good results for certain specific background scenarios, it performs very poorly with respect to LAI (with R^2 of 0.26 ± 0.06 on average individually) in the cases of soil-type and NPV variation. MCARI2 is superior to NDVI, MSR, and sLAIDI because it shows a relatively stable response to LAI over soil backgrounds (with rather small IQR, < 1.5%) and reduced susceptibility to chlorophyll concentration (with S_i < 2%). The MCARI2-LAI relationship is also less sensitive to the variability of soil background reflectance (as evinced by the sd of R^2 < 0.01). These results corroborate the well-established idea that MCARI2 is a significant improvement in monitoring crop LAI for precision agriculture (Haboudane *et al.* 2004).

In comparison with the above discussed LAI-related indices, soil-corrected VIs, including OSAVI and MSAVI respond to LAI with minimal interference of background moisture (this is especially the case for the OSAVI with relatively higher sensitivity, as evinced by the median of S_i with about 52% and IQR of about 1%). Out of the 12 VIs, only OSAVI displays a potential to estimate LAI despite soil-type background variations (R^2 of 0.36 ± 0.004). This result confirms the earlier findings by Thenkabail *et al.* (2000) that the soil-corrected VIs are valuable when remote monitoring of agricultural crops are studied on widely varying soils. However, OSAVI and MSAVI suffer from poor performance, respectively, due to variations introduced by NPV, as confirmed by larger deviations in R^2 (with sd = 0.2 and 0.3, respectively).

4. Discussion

This work is an attempt to unveil variations in the spectral response of two important agronomic variables, namely, C_{ab} and LAI, under various background scenarios. It shows that background optical variability can cause significant deviations in the spectral response to C_{ab} and LAI between different backgrounds and can lead to substantial alterations in the VI- C_{ab}/-LAI correlations.

4.1. Wavelength selection to background optical variability

The use of wavelength selection for chlorophyll or LAI inversion has been well studied. For example, Verrelst et al. (2016a) pointed out that C_{ab} is reasonably well correlated with reflectance at 500, 564, 710, and 714 nm. Zhang *et al.* (2021) suggested the sensitivity wavelengths at 455, 545, 571, 615, 641, 662, 706, 728, and 756 nm for the retrieval of C_{ab}. Concerning LAI, the sensitive spectrum were extracted from the 680 nm and 910 nm (Thenkabail *et al.*, 2002), 740 nm (Horler *et al.*, 1983), 970 nm and 1725 nm (Le Maire *et al.*, 2008) wavelength. Even so, in contrast to earlier findings only analyzing a scenario with a single soil type, our analyses conclude that background optical variability may result in inconsistencies in the specific feature-sensitive wavelengths chosen over different sites (environments and conditions), further supporting the idea of Mitchell *et al.* (2012), who using *in-situ* data figured out the selected wavelengths particularly affected by NPV. As Table 3 shown, the chlorophyll-sensitive peak of canopy spectra in the visible spectral region is observed to have a "blue shift" (towards shorter wavelengths) due to background variability associated with soil-type (the peak located at 560 nm) and NPV (the peak located at 570 nm). In contrast, the peak (at 595 nm) is detected as a "redshift" (towards longer wavelengths) because of background variations linked to moisture contents, whereas the highest sensitivity occurred at 585 nm with a fully absorptive background. The maximum sensitivity of canopy spectra in the red-edge range of 690 to 730 nm shifts toward a longer wavelength only in the cases of soil-type (at 704 nm) and NPV (at 700 nm), as compared to its peak at 695 nm with a fully absorbing background. Consequently, there remains a lack of universality and consistency in the selection of the feature-sensitive wavebands as remote sensing of agriculture frequently involves the measurement of soil and non-vegetation components, which alter plants' spectral characteristics, especially over the semi-arid agricultural landscape where mixed soil-plant litter/residues.

Although the "lambda-by-lambda" band-optimization algorithm could, in principle, determine the sensitive bands for a given experimental dataset (e.g., Thenkabail *et al.*, 2004; Yu *et al.*, 2014), it is suitable merely for field-scale measurements and not for large-scale monitoring. The spectral-band selection using Gaussian process regression (Verrelst et al., 2016a), random forest regression (Liu *et al.*, 2019), and even multi-method ensembles consisting of partial least squares, random forest, and support vector machine regression (Feilhauer *et al.*, 2015) seem more appropriate for band optimizations because of their capacity for band-ranking over very large datasets. Unfortunately, previous band-selection experiments have only put slight emphasis on the effects of variations in the spectral response of canopies with different backgrounds. Appropriate knowledge of background spectra is valuable for accurate discrimination of sensitivity or insensitivity bands from continuous spectra with narrow bandwidth. In future research, the spectral behavior of canopies with various backgrounds such as those given here may serve as *prior* knowledge to select an optimal set of spectral bands and thus improve the estimation of LAI and C_{ab}, particularly using spectral mixture analysis (e.g., Tits *et al.*, 2013) or RTM inversion (e.g., Atzberger *et al.*, 2013).

4.2. Applicability of vegetation indices under various backgrounds

The studied background factors lead to changes in VIs for canopies with the same leaf optical properties and LAI (Barillé *et al.*, 2011). Our analyses further reveal that the impacts of different backgrounds on the VIs' sensitivities, as well as on the relationships between VI and agronomic variables, are highly dependent on the type of background (Fig. 4 and Fig. B).

Compared with other chlorophyll-related indices, the performance of PRI was more strongly influenced by background spectra linked to soil-type variability, followed by NPV. Soil background effects mainly involve two ways (Huete *et al.* 1985): (1) the brightness influences attributed to the variations in soil wetness, and (2) the "color" differences caused by variations of soil background material (e.g., soil type). Our results give an indication that PRI is more susceptible to variations in soil background with contrasting soil types, in agreement with the earlier discussion of Barton and North (2001), which may explain why remote sensing of photosynthesis using PRI over large areas on regional or national scale still remains highly uncertain (Garbulsky *et al.*, 2011). A recent research by Yang (2022) suggested that the combination of NDVI and the soil reflectance at 531 and 570 nm may possibly compensate for the soil background effects on PRI. In addition, Barton and North (2001) also noted that background contributes to PRI for canopies with LAI < 3.0. Our results could not confirm this phenomenon, as it would require an analysis of critical thresholds of vegetation cover corresponding to background effects using LSA, which is beyond the scope of the current study.

Several authors (Main *et al.*,2011) pointed out that a canopy index modified to include the red-edge wavebands was superior to their predecessors with red or NIR band reflectance. However, two red-edge-based spectral indices selected here (i.e., CI_{RE} and MCARI/OSAVI$_{(705,\ 750)}$) performed not as well as expected. One of the reasons for this is that the background reflectance variability could confound the detection of the relatively subtle differences in canopy reflectance due to changes in leaf chlorophyll content (Daughtry *et al.*, 2000). Another explanation is that CI_{RE} and MCARI/OSAVI$_{(705,\ 750)}$ were initially formulated for canopy chlorophyll content variations (Gitelson *et al.*, 2005; Wu *et al.*, 2008), although both indices have also been found to provide accurate leaf-level estimations of foliar chlorophyll content (e.g., Gitelson and Solovchenko, 2017; Stuckens *et al.*, 2011).

In contrast to other chlorophyll-related indices, our analyses show that the MTCI, Macc01 and LICI were highly sensitive to changes in leaf chlorophyll while greatly suppressing the influence of background variability. This confirms previous studies (e.g., Li *et al.*, 2020; Main *et al.*, 2011). However, LAI also interferes with the retrieval of leaf chlorophyll content in the visible and red-edge regions. It has been shown in several studies (e.g., Croft *et al.*, 2020; Qian *et al.*, 2022) that there is a stratification in chlorophyll content (as measured by the MTCI) over regions with sparse- and dense-level vegetation cover due to the strong influence of LAI on MTCI. The LICI might be a plausible candidate for spatially-explicit monitoring of leaf chlorophyll content compared to MTCI over agro-pastoral transitional zones because the former is quite insensitive to both LAI and background variations. Nevertheless, the use of LICI for other vegetation types is yet to be confirmed (Chen *et al.*, 2022) since it was originally developed for wheat and rice (Li *et al.*, 2020). This paper demonstrates the potential of LICI for monitoring applications in wheat-like canopies and over heterogeneous agricultural regions.

In terms of LAI-related VIs, background spectra – especially associated with soil-type and NPV – have been shown to impose more significant effects on NDVI and MSR than on MCARI2 (Fig. 4b) although based on the same narrow bands (i.e., 670 and 800 nm). One possible reason is that the mathematical equations defining MCARI2 could better address the differences in the spectral response of each band under different backgrounds. Given the issue that the most relevant spectral information for LAI estimation varied with soil-type (Darvishzadeh *et al.*, 2008a), it must be carefully considered when the NDVI-/MSR- LAI relationships are applied to imagery where green vegetation, soil-type, NPV components are aggregated. Nonetheless, MCARI2 exhibits a notable discrepancy in the correlations with LAI (as evinced by R^2 with 0.34 ± 0.02) due to the presence of NPV. It thus might be sub-optimum in cases where NPV is a significant and variable component of surface cover. These are interesting findings as earlier studies have mostly disregarded the occurrence of non-photosynthetic materials – particularly the appreciable amounts of standing litter present in no-tillage fields. More real data analysis on the effects of NPV on MCARI2 representing vegetation activity (e.g., LAI) is needed in agricultural applications.

We found that both OSAVI and MSAVI are quite insensitive to soil brightness, relatively insensitive to soil "color" attributed to soil-type, but considerably affected by NPV. Prior studies (e.g., Li *et al.*, 2019) mostly focused on evaluating soil brightness and saturation effects for estimating LAI using soil-corrected VIs. However, aside from soil, the background of a given site consists of litter, crop residues, senescent grass, and sometimes moss. The optical properties of these materials differ greatly from that of the soil. More analysis is thus needed regarding the impact of NPV on soil-corrected VIs in areas with abundant non-photosynthetic materials. Our results imply that, regardless of the robustness of these indices based on the soil line concept (Baret *et al.*, 1993), the background effects of soil-type and NPV cannot be removed entirely.

In conclusion, this research provides a physically-based interpretation of why C_{ab} or LAI retrievals have low accuracy in some study sites (e.g., Pisek *et al.*, 2010). This can be at least partially attributed to the background spectra. To mitigate the effects of background spectral variations in the retrieval of terrestrial vegetation bio-geophysical properties, multi-angle spectral data (Gemmell, 2000) and new VI-correction methods have been recommended. The latter can be based on the fraction of canopy cover (e.g., Li *et al.*, 2016; Van Beek *et al.*, 2015; Yao *et al.*, 2014) or on the fractions of NPV and soil background (Verrelst *et al.*, 2008).

4.3. Potential and Limitations

Numerical experiments based on radiation transfer simulations are essential to understand the spectral response of biophysical and biochemical parameters with different canopy backgrounds (e.g., Malenovský *et al.*, 2008; Vincini *et al.*, 2008). A unique advantage of this modelling is the ability to cover a wide range of scenarios while circumventing uncertainties related to measurement errors (Verrelst *et al.*, 2010). Although the analysis presented here is based on the simulated data, our investigations showed that simulated and ground truth measurements of wheat canopy spectra are generally in good agreement (see Appendix B). These results suggest that our simulations are reliable representations of the contribution of C_{ab} and LAI on wheat-like canopy reflectance. In real-world experiments, explicitly quantifying these dynamic sensitivities is difficult since such wide-ranging and contrasting conditions cannot be easily generated through field campaigns. Our detailed analyses provide a good reference for other research groups studying the impacts of subsets of the backgrounds.

Considering the broad range of simulated vegetation properties (in Table 1), we expect these findings to be useful for remotely sensed monitoring of wheat and other crops with similar canopy structures to wheat (e.g., rice, barley, soybean, etc.). Similarly, as a wide range of background spectra were considered (Fig. 1), many different background effects could be included. Note that, even though the LAI values defined here had a large range (0.1 to 10), due to PROSAIL model without taking into account LAI phenology patterns at specific growth status, it might not present the dynamics of vegetation spectral response to seasonal canopy-background reflectance. A GSA involving coupled crop growth and radiative transfer models (e.g., Thorp *et al.*, 2012) would be a plausible way to evaluate the spectral-temporal behavior of crops to background properties.

Although the contribution of soil to canopy reflectance is often reported to be negligible for LAI > 3 or 4 (Goel, 1988), the results of our study showed that they still affect the crop canopy spectra (Fig. 5, Appendix C). Therefore, it is necessary to consider the spectral response of agronomic variables even in areas with dense vegetation coverage. Fig. 5 also demonstrates the need for a more comprehensive soil spectral library in which for a given soil type, many different water contents have been measured. Due to the lack of such data we had to run simulations for (i) soil type effects, and (ii) soil wetness effects separately from each other, leading to the two distinct sets shown in Fig. 5 with mutually no overlap.

5. Conclusion

Unravelling the spectral response of agronomic variables despite different backgrounds is of fundamental importance for an effective Earth observation (EO)-based monitoring of crop physiological and phenological status. With the availability of spaceborne imaging spectrometers, this need further increases, as researchers and practitioners can now use/optimize subsets of spectral bands for their specific applications. In this respect, we highlighted that the contribution of each parameter to the spectral behavior of wheat-like canopies varies with the optical properties of canopy background, particularly associated with soil-type and NPV whose impacts are more significant than that caused by background moisture.

In terms of remotely-sensed chlorophyll content estimates, our analysis suggests that the canopy reflectance measurements at the 560 and 704 nm are desirable due to their relatively high sensitivity to C_{ab}, with minimum soil impact. On the other hand, the canopy spectra in the interval 774–900 nm is recommended for LAI estimation only for more or less wet background surfaces, while its sensitivity to LAI shows remarkable differences among cases of background soil-type and NPV. Comparing analyses of the sensitivities and correlations of VIs to C_{ab} and LAI for different canopy backgrounds demonstrates that background reflectance variability is a critical factor leading to substantial uncertainties in the estimation of C_{ab} and LAI using EO data. Our analysis points out that LICI, Macc01 and OSAVI, MCARI2 potentially provide better estimates of C_{ab} and LAI, respectively, because of their higher responsiveness to those agronomic variables at a reduced background influence. Notwithstanding, a single spectral index providing a generic algorithm for the two agronomic variables under all "disturbance factors" (comprising soil-type, NPV, irrigated components, etc.), is not realistic. An area-wide canopy background classification based on *a priori* landscape stratification thus seems indispensable for large-scale mapping of leaf chlorophyll content and LAI.

Additionally, our findings help to improve understanding of the subtle changes in the relationships between spectral features and C_{ab} and LAI over various background scenarios, which is one of the fundamental requirements for their successful retrieval via the current generation of hyperspectral satellite sensors (e.g., GF-5/AHSI, PRISMA, EnMAP), and those anticipated in the near future (e.g., CHIME, HISUI), and is thus pivotal for accurately diagnosing crop growth status. Although our findings need to be verified further with real-world experiments and/or actual imageries, this aspect is beyond the scope of the current study and will be addressed in our future studies.

Declaration of Competing Interest

The authors declare that they have no known competing financial interests or personal relationships that could have appeared to influence the work reported in this paper.

Data availability

Data will be made available on request.

Acknowledgement

This research was partly supported by the National Natural Science Foundation of China (No. 42101334, 42101335), and the Natural Science Foundation of Shandong Province (No. ZR2021QD120, ZR2021QD015, ZR2020QD011). The first author especially acknowledges the tremendous amount of feedback of Dr. Jin Xu which has greatly improved the paper. The first author is particularly grateful to Dr. Jean-Baptiste Féret for the fruitful discussions about background effects. The authors warmly thank the two anonymous reviewers for their constructive comments and suggestions.

Appendix A

To further study background effects, the differences of the spectral response of a canopy over scattering backgrounds (shown in Fig. 3) was compared to that over a fully absorbing background (shown in Fig. A). Canopy reflectance in the 550–710 nm spectral region exhibits divergent responses to changes in C_{ab} between scattering backgrounds through comparison with those sensitivities of the totally absorbing background: the S_i is slightly higher (approximately 0–9%) over wet backgrounds and considerably lower (around 0–29%) across contrastive soil-type and NPV. This S_i difference is most pronounced in the red range (660–680 nm), notably with soil-type cases (over 20% lower than those S_i with a completely absorbing

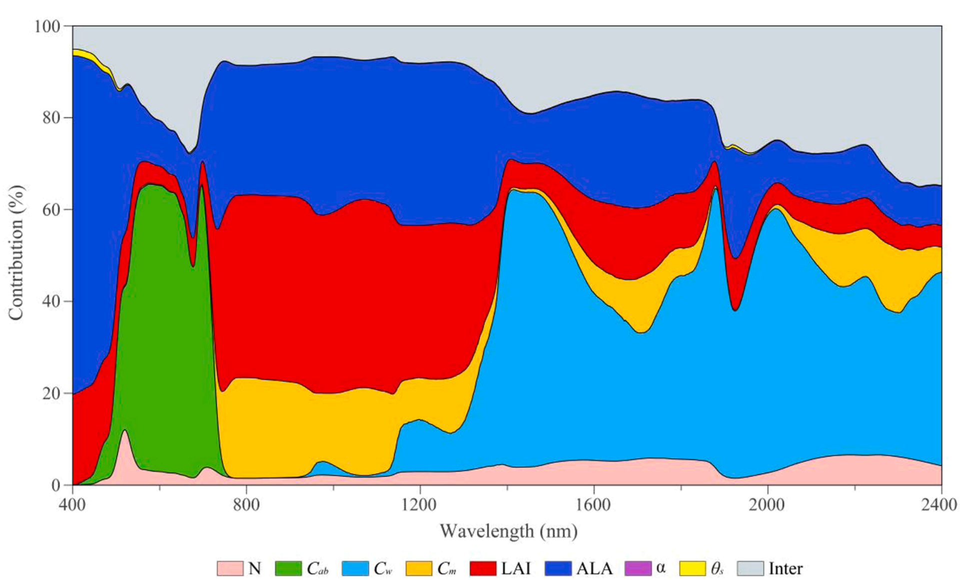

Fig. A. Main effect and interactions of the EFAST sensitivity analysis on vegetation biophysical and biochemical parameters with a totally absorbing background.

background). This result corresponds to early findings that experimental measurements of red reflectance are susceptible to the effects of variable irradiance and background (Curran & Milton, 1983). Besides, equivalent water thickness (C_w) explains about 31%–61% of the canopy reflectance variation in the SWIR wavelength longer than 1880 nm (termed "SWIR2" hereafter) under the zero-background case, much larger than LAI does with a contribution less than 12%. This result is an apparent difference with GSA results only concerning one specific soil background that LAI governed over 50% of the variation in SWIR2, greater than C_w does (e.g., Xiao *et al.* 2014; Verrelst et al., 2015a, 2016b). This inconsistency is tentatively attributed to the fact that the background has a much higher single-scattering albedo in the SWIR2 spectral part than does green vegetation (Asner, 1998), so the SWIR2 reflectance of plant canopy mixed with the background is more sensitive to changes in LAI than that under the zero-background case in the absence of specular reflection. Furthermore, the sensitivity of canopy spectra in the NIR plateau (800–1300 nm) to LAI decreases dramatically while the sensitivity of red reflectance in the wavelength interval [665, 680 nm] and SWIR2 reflectance increases compared to those responsiveness in a totally absorbing background, respectively.

The comparison of the response of VIs over the scattering backgrounds with their "pure" counterparts responsiveness under fully absorbing background (as presented in Fig. B and C) illustrates the performance of the VIs (especially LAI-related indices) could be misleading due to background optical properties. The sensitivity of NDVI to LAI in the zero-background case ($S_i = 7\%$) is far less than that with canopy backgrounds. Theoretically, the NDVI relies on the spectral contrast between red and NIR signatures (Rahman *et al.*, 2004). The NDVI-LAI insensitivity can be accounted for by the fact that the red-NIR contrast is fairly uniform under a 100% absorbing background due to multiple interactions within the canopy only, which is similar to the saturation of NDVI at high values of LAI. This result is in agreement with the findings of Gao *et al.* (2000). While the multiple scattering process in the vegetation background theoretically enhances the response of NDVI to LAI changes and thus the NDVI-LAI relationship has a larger correlation coefficient than that under totally absorbing background ($R^2 = 0.04$). Likewise, the sensitivities and correlations of MSR-LAI and sLAIDI-LAI relationships are found to be larger than that with totally absorbing background ($S_i = 12\%$ and 14%, $R^2 = 0.09$ and 0.11, respectively). Note that this positive contribution of canopy background to spectral response of VIs only is observed for LAI-related VIs including NDVI, MSR, and

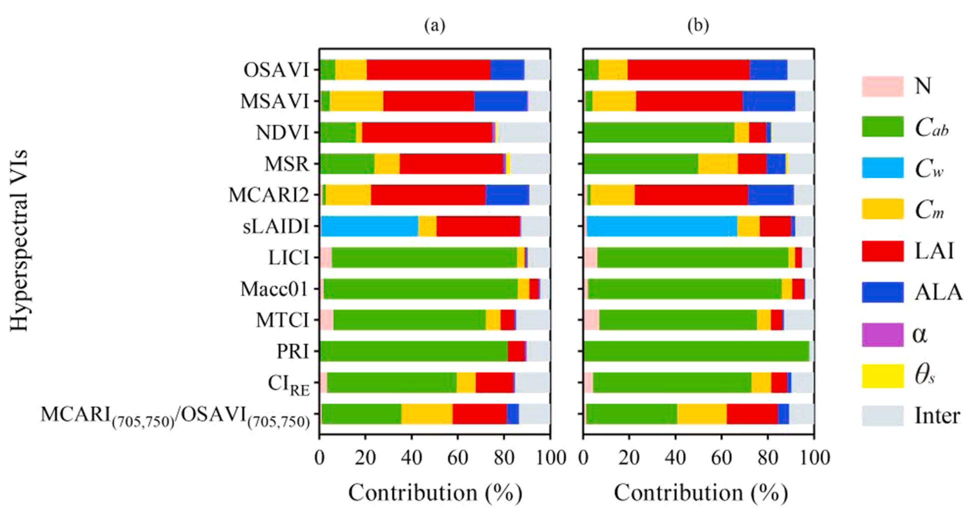

Fig. B. Results of the global sensitivity analysis (the mean values of the first-order sensitivity indices) for each of the selected vegetation indices across (a) scattering and (b) fully absorbing backgrounds.

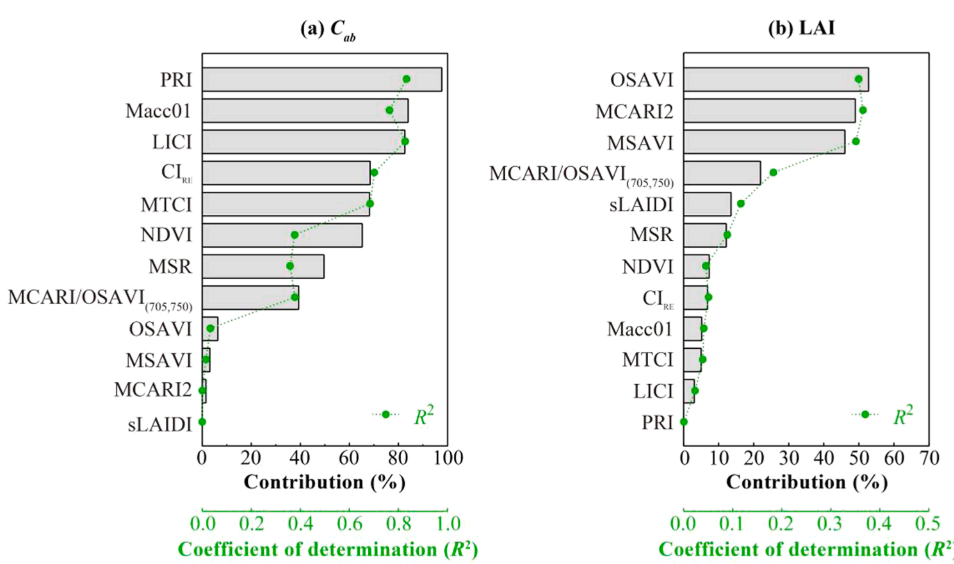

Fig. C. Sensitivity and correlation of VI to (a) C_{ab} and (b) LAI under conditions of a completely absorbing background.

sLAIDI responsiveness to LAI but are rarely found in VIs related to chlorophyll content. Overall, the results of the comparative analysis reveal that the contributions of agronomic variables to plant-canopy spectra depend on wavelength and differ considerably with the background scenarios. Such information is needed to the understanding of the narrowband EO data discerning subtle, but import, features related to plant phenotypes.

Appendix B

The performances of the PROSAIL are evaluated by comparison between measured and simulated reflectance. Similar works also have been carried out by Schlerf and Atzberger (2006) and Darvishzadeh *et al.* (2008b). The results (Fig. D) illustrate a good agreement between the measured and modelled wheat canopy spectra.

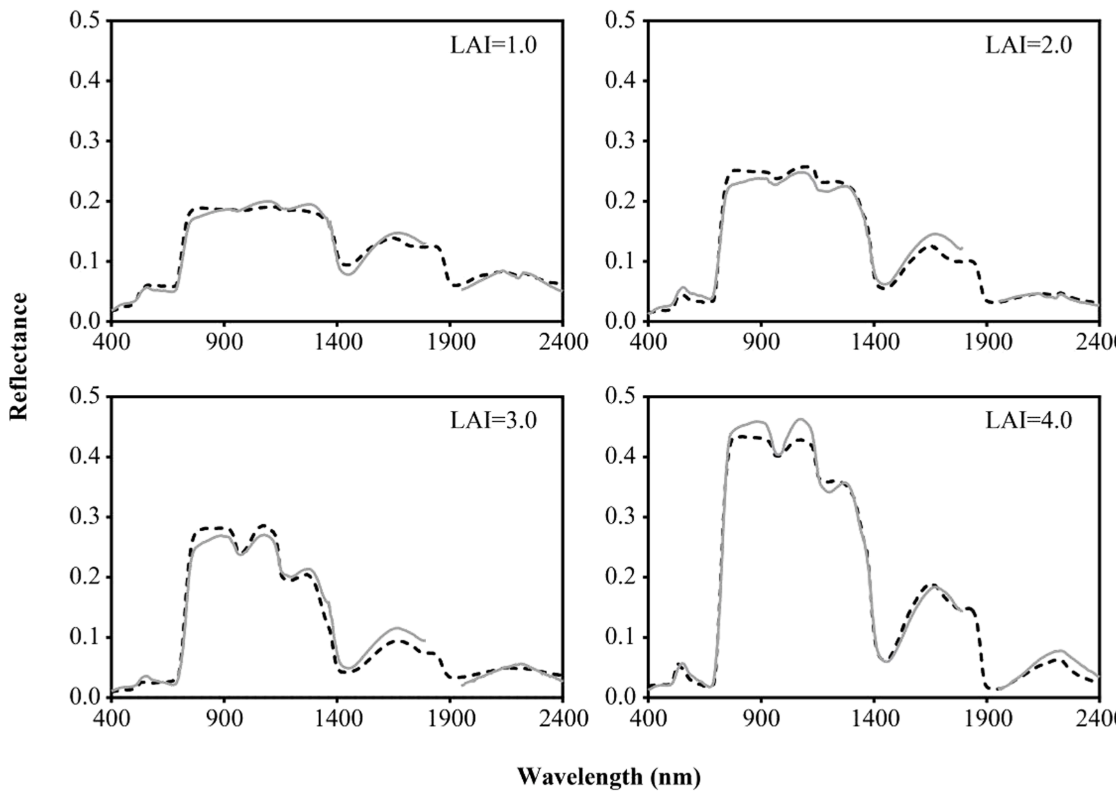

Fig. D. Measured (continuous line) and modelled (dashed black line) wheat canopy reflectance for different values of canopy LAI.

Appendix C

In the literature it is often stated that the contribution of soil to canopy reflectance might be negligible for LAI > 3 or 4. We tested this assumption further in our study through modelling. The relative changes in canopy reflectance (Diff) under different LAI values was calculated based on the equation (Sun *et al.*, 2020):

$$\mathrm{Diff} = \left| \frac{Ref_2 - Ref_1}{Ref_1} \times 100\% \right|$$

where Ref_1 is the simulated canopy reflectance under one background reflectance, while Ref_2 is corresponding reflectance under another background reflectance.

Figs. E and F show that background optical variability continues to influence the canopy reflectance even when LAI $\geq$ 6, even though such subtle differences in canopy reflectance might not be measurable from an optical sensor due to noise etc.

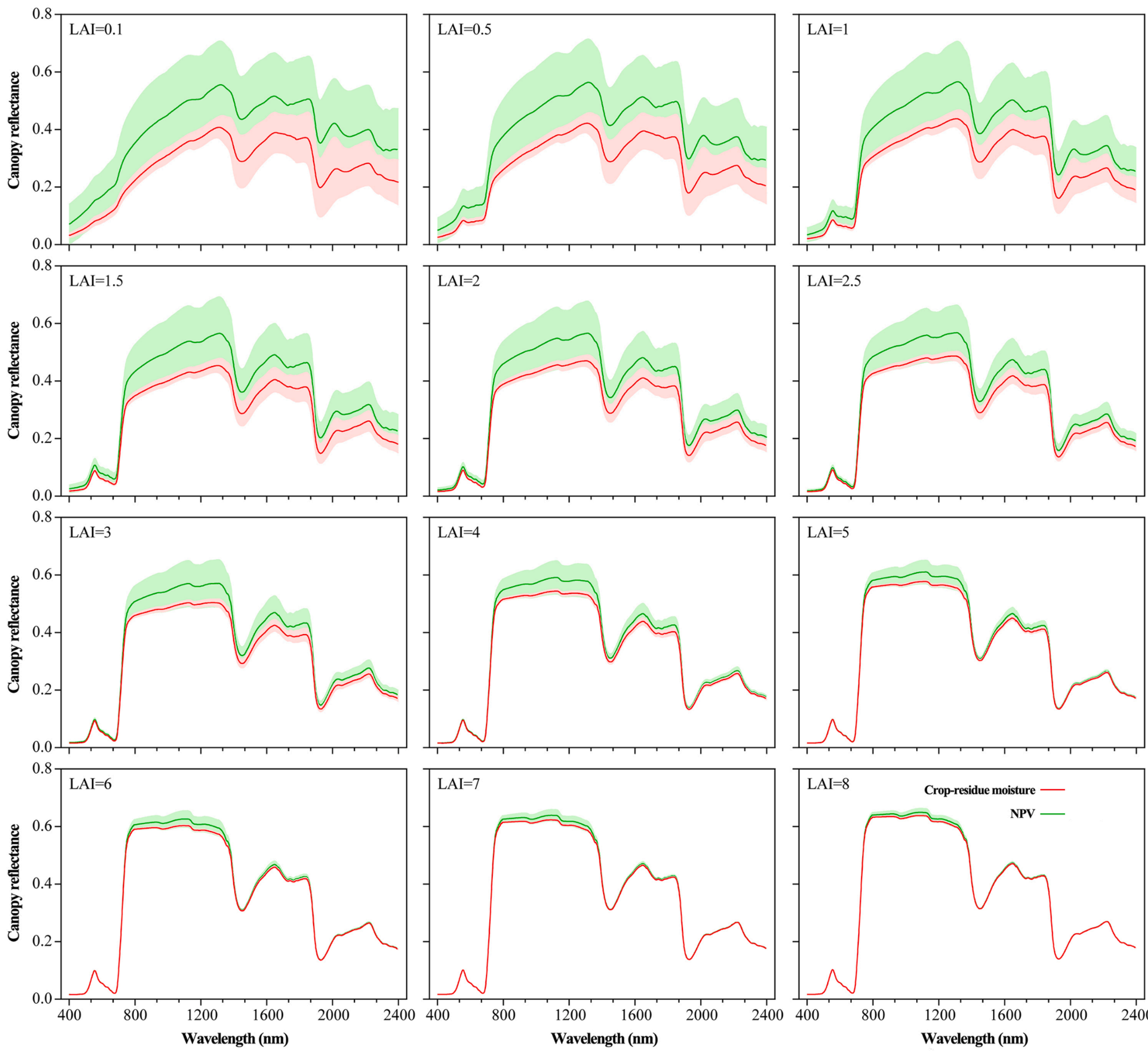

Fig. E. The modelled influences of NPV or crop-residue moisture on canopy reflectance with varying LAI values (LAI = 0.1, 0.5, 1, 1.5, 2, 2.5, 3, 4, 5, 6, 7, 8) based on PROSAIL. The distributions of all other PROSAIL parameters are kept constant (i.e., N = 1.5; $C_{ab} = 25\ \mu g/cm^2$; $C_{xc} = 8\ \mu g/cm^2$; $C_{bp} = 0$; $C_w = 0.01$ cm; $C_m = 0.004$ g $/cm^2$; ALA = 57°; $\theta_s = 37°$), and only the set of background spectra is changed.

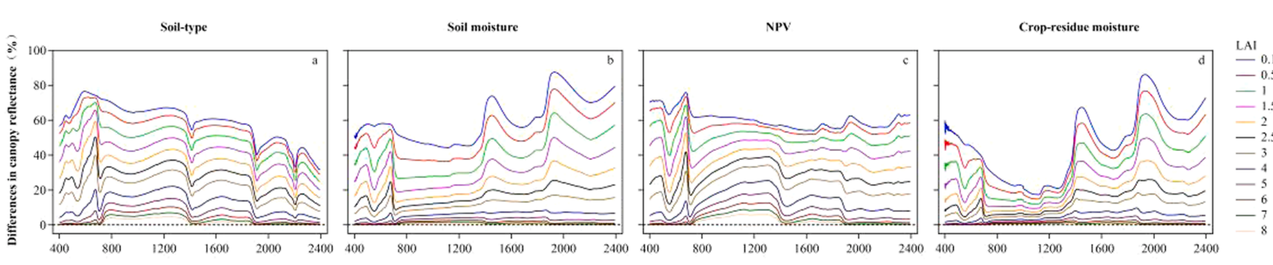

Fig. F. Relative changes in canopy reflectance (Diff) under different LAI values. The horizontal dash line at 0 indicates no differences in reflectance due to background changes.

References

Amin, E., Verrelst, J., Rivera-Caicedo, J.P., Pipia, L., Ruiz-Verdú, A., Moreno, J., 2021. Prototyping sentinel-2 green LAI and brown LAI products for cropland monitoring. Remote Sens. Environ. 255, 112168 https://doi.org/10.1016/j.rse.2020.112168.

Asner, G.P., 1998. Biophysical and biochemical sources of variability in canopy reflectance. Remote Sens. Environ. 64 (3), 234–253. https://doi.org/10.1016/S0034-4257(98)00014-5.

Atzberger, C., Darvishzadeh, R., Schlerf, M., Le Maire, G., 2013. Suitability and adaptation of PROSAIL radiative transfer model for hyperspectral grassland studies. Remote Sens. Lett. 4 (1), 55–64. https://doi.org/10.1080/2150704X.2012.689115.

Bach, H., Verhoef, W., 2003. Sensitivity studies on the effect of surface soil moisture on canopy reflectance using the radiative transfer model GeoSAIL. IEEE Int. Geosci. Remote Sens. Symp. Proc. IEEE 3, 1679–1681. https://dio.org/10.1109/IGARSS.2003.1294215.

Baret, F., Guyot, G., 1991. Potentials and limits of vegetation indices for LAI and APAR assessment. Remote Sens. Environ. 35, 161–173. https://doi.org/10.1016/0034-4257(91)90009-U.

Baret, F., Jacquemoud, S., Hanocq, J.F., 1993. The soil line concept in remote sensing. Remote Sens. Rev. 7, 65–82. https://doi.org/10.1080/02757259309532166.

Barillé, L., Mouget, J., Méléder, V., Rosa, P., Jesus, B., 2011. Spectral response of benthic diatoms with different sediment backgrounds. Remote Sens. Environ. 115, 1034–1042. https://doi.org/10.1016/j.rse.2010.12.008.

Barton, C.V.M., North, P.R.J., 2001. Remote sensing of canopy light use efficiency using the photochemical reflectance index Model and sensitivity analysis. Remote Sens. Environ. 78, 264–273. https://doi.org/10.1016/S0034-4257(01)00224-3.

Berger, K., Atzberger, C., Danner, M., D'Urso, G., Mauser, W., Vuolo, F., et al., 2018. Evaluation of the PROSAIL model capabilities for future hyperspectral model environments: a review study. Remote Sens. (Basel) 10, 85. https://doi.org/10.3390/rs10010085.

Chen, J.M., 1996. Evaluation of vegetation indices and a modified simple ratio for boreal applications. Can. J. Remote Sens. 22, 229–242. https://doi.org/10.1080/07038992.1996.10855178.

Chen, J.M., Ju, W., Ciais, P., Viovy, N., Liu, R., Liu, Y., Lu, X., 2019. Vegetation structural change since 1981 significantly enhanced the terrestrial carbon sink. Nat. Commun. 10, 4259. https://doi.org/10.1038/s41467-019-12257-8.

Chen, J.M., Xu, M., Wang, R., Li, D., Liu, R., Ju, W., et al., 2022. Next step in vegetation remote sensing: synergetic retrievals of canopy structural and leaf biochemical parameters. In: Li, B., Shi, X., Zhu, AX., Wang, C., Lin, H. (Eds.), New Thinking in GIScience. Springer, Singapore. https://doi.org/10.1007/978-981-19-3816-0_23.

Croft, H., Chen, J.M., Luo, X., Ba Rtlett, P., Chen, B., Staebler, R.M., 2017. Leaf chlorophyll content as a proxy for leaf photosynthetic capacity. Glob. Change Biol. 23, 3513–3524. https://doi.org/10.1111/gcb.13599.

Croft, H., Chen, J.M., Wang, R., Mo, G., Luo, S., Luo, X., et al., 2020. The global distribution of leaf chlorophyll content. Remote Sens. Environ. 236, 111479 https://doi.org/10.1016/j.rse.2019.111479.

Curran, P.J., Milton, E.J., 1983. The relationships between the chlorophyll concentration, LAI and reflectance of a simple vegetation canopy. Int. J. Remote Sens. 4 (2), 247–255. https://doi.org/10.1080/01431168308948544.

Darvishzadeh, R., Skidmore, A., Abdullah, H., Cherenet, E., Ali, A., Wang, T., et al., 2019. Mapping leaf chlorophyll content from Sentinel-2 and RapidEye data in spruce stands using the invertible forest reflectance model. Int. J. Appl. Earth Obs. Geoinf. 79, 58–70. https://doi.org/10.1016/j.jag.2019.03.003.

Darvishzadeh, R., Skidmore, A., Atzberger, C., Wieren, S., 2008a. Estimation of vegetation LAI from hyperspectral reflectance data: effects of soil types and plant architecture. Int. J. Appl. Earth Obs. Geoinf. 10, 358–373. https://doi.org/10.1016/j.jag.2008.02.005.

Darvishzadeh, R., Skidmore, A., Schlerf, M., Atzberger, C., 2008b. Inversion of a radiative transfer model for estimating vegetation LAI and chlorophyll in a heterogeneous grassland. Rem. Sens. Environ. 112, 2592–2604. https://doi.org/10.1016/j.rse.2007.12.003.

Dash, J., Curran, P.J., 2004. The MERIS terrestrial chlorophyll index. Int. J. Remote Sens. 25, 5403–5413. https://doi.org/10.1080/0143116042000274015.

S., T. Daughtry, C., Walthall, C.L., Kim, M.S., de Colstoun, E.B., McMurtrey III, J.E., 2000. Estimating corn leaf chlorophyll concentration from leaf and canopy reflectance Remote Sens. Environ. 74 (2), 229–239. https://doi.org/10.1016/S0034-4257(00)00113-9.

Delalieux, S., Somers, B., Hereijgers, S., Verstraeten, W.W., Keulemans, W., Coppin, P., 2008. A near-infrared narrow-waveband ratio to determine leaf area index in orchards. Remote Sens. Environ. 112, 3762–3772. https://doi.org/10.1016/j.rse.2008.05.003.

Díaz, B.M., Blackburn, G.A., 2003. Remote sensing of mangrove biophysical properties: evidence from a laboratory simulation of the possible effects of background variation on spectral vegetation indices. Int. J.Remote Sens. 24 (1), 53–73. https://doi.org/10.1080/01431160305012.

Dong, T., Liu, J., Shang, J., Qian, B., He, L., Liu, J., et al., 2020. Estimating crop biomass using leaf area index derived from Landsat 8 and Sentinel-2 data. ISPRS J. Photogramm. Remote Sens. 168, 236–250. https://doi.org/10.1016/j.isprsjprs.2020.08.003.

Eitel, J., Long, D.S., Gessler, P.E., Hunt, E.R., Brown, D.J., 2009. Sensitivity of ground-based remote sensing estimates of winter chlorophyll content to variation in soil reflectance. Soil Sci. Soc. Am. J. 73, 1715–1723. https://doi.org/10.2136/sssaj2008.0288.

Fang, H., Baret, F., Plummer, S., Schaepman-Strub, G., 2019. An overview of global leaf area index (LAI): methods, products, validation, and applications. Rev. Geophys. 57 https://doi.org/10.1029/2018RG000608.

Feihauer, H., Asner, G.P., Martin, R.E., 2015. Multi-method ensemble selection of spectral bands related to leaf biochemistry. Remote Sens. Environ. 164, 57–65. https://doi.org/10.1016/j.rse.2015.03.033.

Feret, J.B., François, C., Gitelson, A., Asner, G.P., Barry, K.M., Panigada, C., et al., 2011. Optimizing spectral indices and chemometric analysis of leaf chemical properties using radiative transfer modeling. Remote Sens. Environ. 115, 2742–2750. https://doi.org/10.1016/j.rse.2011.06.016.

Gamon, J.A., Peñuelas, J., Field, C.B., 1992. A narrow-waveband spectral index that tracks diurnal changes in photosynthetic efficiency. Remote Sens. Environ. 41, 35–44. https://doi.org/10.1016/0034-4257(92)90059-S.

Gao, X., Huete, A.R., Ni, W., Miura, T., 2000. Optical-biophysical relationships of vegetation spectra without background contamination. Remote Sens. Environ. 74, 609–620. https://doi.org/10.1016/S0034-4257(00)00150-4.

Garbulsky, M.F., Peñuelas, J., Gamon, J., Inoue, Y., Filella, I, 2011. The photochemical reflectance index (PRI) and the remote sensing of leaf, canopy and ecosystem radiation use efficiencies: a review and meta-analysis. Remote Sens. Environ. 115 (2), 281–297. https://doi.org/10.1016/j.rse.2010.08.023.

Garrity, D., & Bindraban, P. (2004). A globally distributed soil spectral library visible near infrared diffuse reflectance spectra. *ICRAF (World Agroforestry Centre)/ISRIC (World Soil Information) Spectral Library: Nairobi, Kenya*.

Gemmell, F., 2000. Testing the utility of multi-angle spectral data for reducing the effects of background spectral variations in forest reflectance model inversion. Remote Sens. Environ. 72 (1), 46–63. https://doi.org/10.1016/S0034-4257(99)00091-7.

Gitelson, A.A., Keydan, G.P., Merzlyak, M., 2006. Three-band model for noninvasive estimation of chlorophyll, carotenoids, and anthocyanin contents in higher plant leaves. Geophys. Res. Lett. 33, L11402. https://doi.org/10.1029/2006GL026457.

Gitelson, A.A., Solovchenko, A., 2017. Generic algorithms for estimating foliar pigment content. Geophys. Res. Lett. 44, 9293–9298. https://doi.org/10.1002/2017GL074799.

Gitelson, A.A., Viña, A., Arkebauer, T.J., Rundquist, D.C., Keydan, G., Leavitt, B., 2003. Remote estimation of leaf area index and green leaf biomass in maize canopies. Geophys. Res. Lett. 30, 1248. https://doi.org/10.1029/2002GL016450.

Gitelson, A.A., Viña, A., Ciganda, V., Rundquist, D., Arkebauer, T.J., 2005. Remote estimation of canopy chlorophyll content in crops. Geophys. Res. Lett. 32, L08403. https://doi.org/10.1029/2005GL022688.

Goel, N.S., 1988. Models of vegetation canopy reflectance and their use in estimation of biophysical parameters from reflectance data. Remote Sens. Rev. 4, 1–212. https://doi.org/10.1080/02757258809532105.

Gu, C., Du, H., Mao, F., Han, N., Zhou, G., Xu, X., et al., 2016. Global sensitivity analysis of PROSAIL model parameters when simulating Moso bamboo forest canopy reflectance. Int. J. Remote Sens. 37, 5270–5286. https://doi.org/10.1080/01431161.2016.1239287.

Haboudane, D., Miller, J.R., Pattey, E., Zarco-Tejada, P.J., Strachan, I.B., 2004. Hyperspectral vegetation indices and novel algorithms for predicting green LAI of crop canopies: modeling and validation in the context of precision agriculture. Remote Sens. Environ. 90, 337–352. https://doi.org/10.1016/j.rse.2003.12.013.

N., H. Horler, D., Dockray, M., Barber, J, 1983. The red edge of plant leaf reflectance Int. J. Remote Sens. 4 (2), 273–288. https://doi.org/10.1080/01431168308948546.

Houborg, R., Cescatti, A., Migliavacca, M., Kustas, W.P., 2013. Satellite retrievals of leaf chlorophyll and photosynthetic capacity for improved modeling of GPP. Agric. For. Meteorol. 177, 10–23. https://doi.org/10.1016/j.agrformet.2013.04.006.

Huang, J., Tian, L., Liang, S., Ma, H., Becker-Reshef, I., Huang, Y., et al., 2015. Improving winter wheat yield estimation by assimilation of the leaf area index from Landsat TM and MODIS data into the WOFOST model. Agric. For. Meteorol. 204, 106–121. https://doi.org/10.1016/j.agrformet.2015.02.001.

Huete, A.R., 1988. A soil adjusted vegetation index (SAVI). Remote Sens. Environ. 25, 295–309. https://doi.org/10.1016/0034-4257(88)90106-X.

Huete, A.R., Jackson, R.D., Post, D.F., 1985. Spectral response of a plant canopy with different soil background. Remote Sens. Environ. 17 (1), 37–53. https://doi.org/10.1016/0034-4257(85)90111-7.

Huete, A.R., Tucker, C.J., 1991. Investigation of soil influences in AVHRR red and near-infrared vegetation index imagery. Int. J. Remote Sens. 12 (6), 1223–1242. https://doi.org/10.1080/01431169108929723.

Jacquemoud, S., Verhoef, W., Baret, F., Bacour, C., Zarco-Tejada, P.J., Asner, G.P., et al., 2009. PROSPECT+SAIL models: a review of use of vegetation characterization. Remote Sens. Environ. 113, S56–S66. https://doi.org/10.1016/j.rse.2008.01.026.

Jia, K., Liang, S., Gu, X., Baret, F., Wei, X., Wang, X., et al., 2016. Fractional vegetation cover estimation algorithm for Chinese GF-1 wide field view data. Remote Sens. Environ. 177, 184–191. https://doi.org/10.1016/j.rse.2016.02.019.

Jin, X., Li, Z., Nie, C., Xu, X., Feng, H., Guo, W., Wang, J., 2018. Parameter sensitivity analysis of the AquaCrop model based on extended fourier amplitude sensitivity under different agro-meteorological conditions and application. Field Crops Res. 226, 1–15. https://doi.org/10.1016/j.fcr.2018.07.002.

Knipling, E.B., 1970. Physical and physiological basis for the reflectance of visible and near-infrared radiation from vegetation. Remote Sens. Environ. 1 (3), 155–159. https://doi.org/10.1016/S0034-4257(70)80021-9.

Kruse, F.A., Lefkoff, A.B., Boardman, J.W., Heidebrecht, K.B., Shapiro, A.T., Barloon, P. J., Goetz, A.F.H., 1993. The spectral image processing system (SIPS)—interactive visualization and analysis of imaging spectrometer data. Remote Sens. Environ. 44, 145–163. https://doi.org/10.1016/0034-4257(93)90013-N.

Le Maire, G., François, C., Soudani, K., Berveiller, D., Pontailler, J., Bréda, N., et al., 2008. Calibration and validation of hyperspectral indices for the estimation of broadleaved forest leaf chlorophyll content, leaf mass per area, leaf area index and leaf canopy biomass. Remote Sens. Environ. 112 (10), 3846–3864. https://doi.org/10.1016/j.rse.2008.06.005.

Li, D., Chen, J.M., Zhang, X., Yan, Y., Zhu, J., Zheng, H., et al., 2020. Improved estimation of leaf chlorophyll content of row crops from canopy reflectance spectra through minimizing canopy structural effects and optimizing off-noon observation time. Remote Sens. Environ. 248, 111985 https://doi.org/10.1016/j.rse.2020.111985.

Li, F., Zeng, Y., Luo, J., Ma, R., Wu, B., 2016. Modeling grassland aboveground biomass using a pure vegetation index. Ecol. Indic. 62, 279–288. https://doi.org/10.1016/j.ecolind.2015.11.005.

Li, H., Coburn, C.A., Wang, Z.J., Wei, F., Guo, T.C., 2019. Reduced prediction saturation and view effects for estimating the leaf area index of winter wheat. IEEE Trans. Geosci. Remote Sens. 57, 1637–1652. https://doi.org/10.1109/TGRS.2018.2868138.

Li, Y., Demetriades-Shah, T.H., Kanemasu, E.T., Shultis, J.K., Kirkham, M.B., 1993. Use of second derivatives of canopy reflectance for monitoring prairie vegetation over different soil background. Remote Sens. Environ. 44 (1), 81–87. https://doi.org/10.1016/0034-4257(93)90104-6.

Liang, L., Di, L., Zhang, L., Deng, M., Qin, Z., Zhao, S., Lin, H., 2015. Estimation of crop LAI using hyperspectral vegetation indices and a hybrid inversion method. Remote Sens. Environ. 165, 123–134. https://doi.org/10.1016/j.rse.2015.04.032.

Liu, J., Pattey, E., Jégo, G., 2012. Assessment of vegetation indices for regional crop green LAI estimation from Landsat images over multiple growing seasons. Remote Sens. Environ. 123, 347–358. https://doi.org/10.1016/j.rse.2012.04.002.

Liu, Q., Huete, A., 1995. A feedback based modification of the NDVI to minimize canopy background and atmospheric noise. IEEE Trans. Geosci. Remote Sens. 33 (2), 457–465. https://dio.org/10.1109/TGRS.1995.8746027.

Liu, X., Guanter, L., Liu, L., Damm, A., Malenovský, Z., Rascher, U., et al., 2019. Downscaling of solar-induced chlorophyll fluorescence from canopy level to photosystem level using a random forest model. Remote Sens. Environ. 231, 110772 https://doi.org/10.1016/j.rse.2018.05.035.

Ma, B., Li, J., Fan, W., Ren, H., Xu, X., Cui, Y., Peng, J., 2018. Application of an LAI inversion algorithm based on the unified model of canopy bidirectional reflectance distribution function to the Heihe River Basin. J. Geophys. Res. Atmos. 123 (18) https://doi.org/10.1029/2018JD028415, 10,671-10,687.

Maccioni, A., Agati, G., Mazzinghi, P., 2001. New vegetation indices for remote measurement of chlorophylls based on leaf directional reflectance spectra. J. Photochem. Photobiol. B 61, 52–61. https://doi.org/10.1016/S1011-1344(01)00145-2.

Main, R., Cho, M.A., Mathieu, R., O'Kennedy, M.M., Ramoelo, A., Koch, S, 2011. An investigation into robust spectral indices for leaf chlorophyll estimation. ISPRS J. Photogramm. Remote Sens. 66 (6), 751–761. https://doi.org/10.1016/j.isprsjprs.2011.08.001.

Malenovský, Z., Martin, E., Homolová, L., Gastellu-Etchegorry, J.P., Zurita-Milla, R., Schaepman, M.E., et al., 2008. Influence of woody elements of a Norway spruce canopy on nadir reflectance simulated by the DART model at very high spatial resolution. Remote Sens. Environ. 112 (1), 1–18. https://doi.org/10.1016/j.rse.2006.02.028.

Meerdink, S.K., Hook, S.J., Roberts, D.A., Abbott, E.A., 2019. The ECOSTRESS spectral library version 1.0. Remote Sens. Environ. 230, 111196 https://doi.org/10.1016/j.rse.2019.05.015.

J.F.T. Mitchell, J., Glenn, N., Sankey, T., Derryberry, D.R., Germino, M.J., 2012. Remote sensing of sagebrush canopy nitrogen Remote Sens. Environ. 124, 217–223. https://doi.org/10.1016/j.rse.2012.05.002.

Morcillo-Pallarés, P., Rivera-Caicedo, J.P., Belda, S., Grave, C.D., Burriel, H., Moreno, J., Verrelst, J., 2019. Quantifying the robustness of vegetation indices through global sensitivity analysis of homogeneous and forest leaf-canopy radiative transfer models. Remote Sens. (Basel) 11, 2418. https://doi.org/10.3390/rs11202418.

Mousivand, A., Menenti, M., Gorte, B., Verhoef, W., 2014. Global sensitivity analysis of the spectral radiance of a soil-vegetation system. Remote Sens. Environ. 145, 131–144. https://doi.org/10.1016/j.rse.2014.01.023.

M. Pisek, J., Chen, J., Alikas, K., Deng, F, 2010. Impacts of including forest understory brightness and foliage clumping information from multiangular measurements on leaf area index mapping over North America J. Geophys. Res. Biogeosci. 115, G03023. https://doi.org/10.1029/2009JG001138.

Qi, J., Chehbouni, A., Huete, A.R., Kerr, Y.H., Sorooshian, S., 1994. A modified soil adjusted vegetation index. Remote Sens. Environ. 48, 119–126. https://doi.org/10.1016/0034-4257(94)90134-1.

Qian, B., Ye, H., Huang, W., Xie, Q., Pan, Y., Xing, N., et al., 2022. A sentinel-2-based triangular vegetation index for chlorophyll content estimation. Agric. For. Meteorol. 322, 109000 https://doi.org/10.1016/j.agrformet.2022.109000.

Quemada, M., Daughtry, C.S.T., 2016. Spectral indices to improve crop residue cover estimation under varying moisture conditions. Remote Sens. (Basel) 8, 660. https://doi.org/10.3390/rs8080660.

Rahman, M.R., Islam, A.H.M.H., Rahman, M.A., 2004. NDVI derived sugarcane area identification and crop condition assessment. Plan Plus 1 (2), 1–12.

Rondeaux, G., Steven, M., Baret, F., 1996. Optimization of soil-adjusted vegetation indices. Remote Sens. Environ. 55, 95–107. https://doi.org/10.1016/0034-4257(95)00186-7.

Rouse, J.W., Haas, R.H., Schell, J.A., 1974. In: Deering Proceedings of the Third Earth Resources Technology Satellite-1 Symposium. Greenbelt, MD. NASA, pp. 301–317.

Saltelli, A., Annoni, P., 2010. How to avoid a perfunctory sensitivity analysis. Environ. Modell. Softw. 24, 1508–1517. https://doi.org/10.1016/j.envsoft.2010.04.012.

Saltelli, A., Annoni, P., Azzini, I., Campolongo, F., Ratto, M., Tarantola, S., 2010. Variance based sensitivity analysis of model output. Design and estimator for the total sensitivity index. Comput. Phys. Commun. 181, 259–270. https://doi.org/10.1016/j.cpc.2009.09.018.

Saltelli, A., Ratto, M., Andres, T., Campolongo, F., Cariboni, J., Gatelli, D., Saisana, M., Tarantola, S., 2008. Global Sensitivity Analysis: the Primer. John Wiley & Sons.

Schlerf, M., Atzberger, C., 2006. Inversion of a forest reflectance model to estimation structural canopy variables from hyperspectral remote sensing data. Remote Sens. Environ. 100, 281–294. https://doi.org/10.1016/j.rse.2005.10.006.

Shabanov, N.V., Knyazikhin, Y., Baret, F., Myneni, R.B., 2000. Stochastic modeling of radiation regime in discontinuous vegetation canopies. Remote Sens. Environ. 74, 125–144. https://doi.org/10.1016/S0034-4257(00)00128-0.

Shi, Z., Wang, Q., Peng, J., Ji, W., Liu, H., Li, X., Rossel, R.A.V., 2014. Development of a national VNIR soil-spectral library for soil classification and prediction of organic matter concentrations. Sci. China Earth Sci. 57, 1671–1680. https://doi.org/10.1007/s11430-013-4808-x.

SIMLAB, 2009. Version 2.2, simulation environment for uncertainty and sensitivity analysis. Dev. Joint Res. Centre Eur. Commiss. http://simlab.jrc.ec.euro.

Stuckens, J., Dzikiti, S., Verstraeten, W.W., Verreynne, S., Swennen, R., Coppin, P, 2011. Physiological interpretation of a hyperspectral time series in a citrus orchard. Agric. For. Meteorol. 151, 1002–1015. https://doi.org/10.1016/j.agrformet.2011.03.006.

Sun, Y., Qi, Q., Ren, H., Zhang, T., Chen, S., 2020. Red-edge band vegetation indices for leaf area index estimation from Sentinel-2/MSI imagery. IEEE Trans. Geosci. Remote Sens. 58, 826–840. https://doi.org/10.1109/TGRS.2019.2940826.

Thenkabail, P.S., Enclona, E.A., Ashton, M.S., Legg, C., De Dieu, M.J, 2004. Hyperion, IKONOS, ALI, and ETM+ sensors in the study of African rainforests. Remote Sens. Environ. 90, 23–43. https://doi.org/10.1016/j.rse.2003.11.018.

Thenkabail, P.S., Smith, R.B., Pauw, E.D., 2000. Hyperspectral vegetation indices and their relationships with agricultural crop characteristics. Remote Sens. Environ. 71, 158–182. https://doi.org/10.1016/S0034-4257(99)00067-X.

Thenkabail, P.S., Smith, R.B., Pauw, E.D., 2002. Evaluation of narrowband and broadband vegetation indices for determining optimal hyperspectral wavebands for agricultural crop characterization. Photogramm. Eng. Remote Sens. 68 (6), 607–622.

Thorp, K.R., Wang, G., West, A.L., Moran, M.S., Bronson, K.F., White, J.W., et al., 2012. Estimating crop biophysical properties from remote sensing data by inverting linked radiative transfer and ecophysiological models. Remote Sens. Environ. 124, 224–233. https://doi.org/10.1016/j.rse.2012.05.013.

Tits, L., Somers, B., Stuckens, J., Farifteh, J., Coppin, P., 2013. Integration of in situ measured soil status and remotely sensed hyperspectral data to improve plant production system monitoring: concept, perspectives and limitations. Remote Sens. Environ. 128, 197–211. https://doi.org/10.1016/j.rse.2012.10.006.

Van Beek, J., Tits, L., Somers, B., Deckers, T., Janssens, P., Coppin, P., 2015. Reducing background effects in orchards through spectral vegetation index correction. Int. J. Appl. Earth Obs. Geoinf. 24, 167–177. https://doi.org/10.1016/j.jag.2014.08.009.

Verger, A., Vigneau, N., Chéron, C., Gilliot, J.M., Comar, A., Baret, F., 2014. Green area index from an unmanned aerial system over wheat and rapeseed crops. Remote Sens. Environ. 152, 654–664. https://doi.org/10.1016/j.rse.2014.06.006.

Verrelst, J., Rivera, J.P., Gitelson, A., Delegido, J., Moreno, J., Camps-Valls, G., 2016a. Spectral band selection for vegetation properties retrieval using Gaussian processes regression. Int. J. Appl. Earth Obs. Geoinf. 52, 554–567. https://doi.org/10.1016/j.jag.2016.07.016.

Verrelst, J., Rivera, J.P., van der Tol, C., Magnani, F., Mohammed, G., Moreno, J., 2015a. Global sensitivity analysis of the SCOPE model: what drives simulated canopy-leaving sun-induced fluorescence? Rem. Sens. Environ. 166, 8–21. https://doi.org/10.1016/j.rse.2015.06.002.

Verrelst, J., Schaepman, M.E., Koetz, B., Kneubühler, M., 2008. Angular sensitivity analysis of vegetation indices derived from CHRIS/PROBA data. Remote Sens. Environ. 112 (5), 2341–2353. https://doi.org/10.1016/j.rse.2007.11.001.

Verrelst, J., Schaepman, M.E., Malenovský, Z., Clevers, J.G.P.W., 2010. Effects of woody elements on simulated canopy reflectance: implications for forest chlorophyll content retrieval. Remote Sens. Environ. 114, 647–656. https://doi.org/10.1016/j.rse.2009.11.004.

Vincini, M., Frazzi, E., D'Alessio, 2008. A broad-band leaf chlorophyll vegetation index at the canopy scale. Precis. Agric. 9, 303–319. https://doi.org/10.1007/s11119-008-9075-z.

Wang, S., Yang, D., Li, Z., Liu, L., Huang, C., Zhang, L., 2019. A global sensitivity analysis of commonly used satellite-derived vegetation indices for homogeneour canopies based on model simulation and random forest learning. Remote Sens. (Basel) 11, 2547. https://doi.org/10.3390/rs11212547.

Widlowski, J.L., Mio, C., Disney, M., Adams, J., Andredakis, I., Atzberger, C., et al., 2015. The fourth phase of the radiative transfer model intercomparison (RAMI) exercise: actual canopy scenarios and conformity testing. Remote Sens. Environ. 169, 418–437. https://doi.org/10.1016/j.rse.2015.08.016.

Wu, C., Niu, Z., Tang, Q., Huang, W., 2008. Estimating chlorophyll content from hyperspectral vegetation indices: modeling and validation. Agric. For. Meteorol. 148, 1230–1241. https://doi.org/10.1016/j.agrformet.2008.03.005.

Xiao, Y., Zhao, W., Zhou, D., Gong, H., 2014. Sensitivity analysis of vegetation reflectance to biochemical and biophysical variables at leaf, canopy, and regional scales. IEEE Trans. Geosci. Remote Sens. 52, 4014–4024. https://doi.org/10.1109/TGRS.2013.2278838.

Xu, D., An, D., Guo, X., 2020. The impact of non-photosynthetic vegetation on LAI estimation by NDVI in mixed grassland. Remote Sens. (Basel) 12, 1979. https://dio.org/10.3390/rs12121979.

Xu, J., Meng, J., Quackenbush, L.J., 2019a. Use of remote sensing to predict the optimal harvest date of corn. Field Crops Research 236, 1–13. https://doi.org/10.1016/j.fcr.2019.03.003.

Xu, M., Liu, R., Chen, J.M., Liu, Y., Shang, R., Ju, W., et al., 2019b. Retrieving leaf chlorophyll content using a matrix-based vegetation index combination approach.

Remote Sensing of Environment 224, 60–73. https://doi.org/10.1016/j.rse.2019.01.039.
Yang, P., 2022. Exploring the interrelated effects of soil background, canopy structure and sun-observer geometry on canopy photochemical reflectance index. Remote Sens. Environ. 279, 113133 https://doi.org/10.1016/j.rse.2022.113133.
Yao, X., Ren, H., Cao, Z., Tian, Y., Cao, W., Zhu, Y., Cheng, T., 2014. Detecting leaf nitrogen content in wheat with canopy hyperspectrum under different soil backgrounds. Int. J. Appl. Earth Obs. Geoinf. 32, 114–124. https://doi.org/10.1016/j.jag.2014.03.014.
Yu, K., Lenz-Wiedemann, V., Chen, X., Bareth, G., 2014. Estimating leaf chlorophyll of barley at different growth stages using spectral indices to reduce soil background and canopy structure effects. ISPRS J. Photogramm. Remote Sens. 97, 58–77. https://doi.org/10.1016/j.isprsjprs.2014.08.005.
Zhang, L., Guo, C.L., Zhao, L.Y., Zhu, Y., Cao, W.X., Tian, Y.C., et al., 2016. Estimating wheat yield by integrating the WheatGrow and PROSAIL models. Field Crops Res. 192, 55–66. https://doi.org/10.1016/j.fcr.2016.04.014.
Zhang, Y., Hui, J., Qin, Q., Sun, Y., Zhang, T., Sun, H., Sun, H., 2021. Transfer-learning-based approach for leaf chlorophyll content estimation of winter wheat from hyperspectral data. Remote Sens. Environ., 112724 https://doi.org/10.1016/j.rse.2021.112724.